The Degradation Mechanisms of Nickel Metal-Hydride Battery and Lead Acid Battery during Open Circuit

Taichi Iwai

Department of Fundamental Energy Science

Graduate School of Energy Science

Kyoto University

2018

Table of Contents

Chapter 1 Introduction

1.1 Nickel Metal-Hydride Battery

1.1.1 Overview of Nickel Metal-Hydride Battery

Nickel metal-hydride battery has been widely used from small- to large-scaled applications for digital cameras, personal computers, or hybrid vehicles since it has been invented in 1970s [1]. In the secondary batteries, nickel metal-hydride battery has the relatively high capacity and is stable for the large current discharge operation. As the secondary battery using nickel oxyhydroxide, nickel cadmium battery had been widely used. Nickel metal-hydride battery has the same cathode and electrolyte as nickel cadmium battery, but hydrogen absorbing alloy is used for the anode material because cadmium (anode material of nickel cadmium battery) has the environmental loading and should be removed.

1.1.2 Electrode Materials of Nickel Metal-Hydride Battery

For the electrode materials of nickel metal-hydride battery, nickel oxyhydroxide and hydrogen absorbing alloy are used for the cathode and anode active materials, respectively. 9M potassium hydroxide solution is used as electrolyte. Electrochemical reactions for nickel metal-hydride battery are shown below. Nickel metal-hydride battery can be regarded as the battery to utilize the reversible proton transfer.

$$\text{Cathode: } NiOOH + H_2O + e^- \rightleftarrows Ni(OH)_2 + OH^-$$

$$\text{Anode: } MH + OH^- \rightleftarrows M + H_2O + e^-$$

※ M represents the hydrogen absorbing alloy. Right direction describes discharge reaction and left direction describes charge reaction.

1.1.3 Nickel Oxyhydroxide

For the cathode active material of nickel metal-hydride battery, nickel oxyhydroxide (NiOOH) is used. NiOOH has the two polymorphs, i.e. β-phase and γ-phase [2]. β-phase

is categorized as hexagonal crystal, although the crystal structure of γ-phase has not been clarified yet. Bode's diagram [3-11] for NiOOH is shown in Fig. 1-1. At the discharged state, cathode active material exists as β-$Ni(OH)_2$. When β-$Ni(OH)_2$ is charged, it transforms into β-NiOOH. But when β-$Ni(OH)_2$ is overcharged and desorption of proton occurs to some extent, β-NiOOH transforms into γ-NiOOH. And due to the less stability of α-$Ni(OH)_2$ in the potassium hydroxide solution, it transforms into γ-NiOOH immediately [3]. The difference between β-NiOOH and γ-NiOOH is mainly detected by XRD measurement. γ-NiOOH has the characteristic peak in $2\theta = 10 \sim 15°$, which is not observed for β-NiOOH [12].

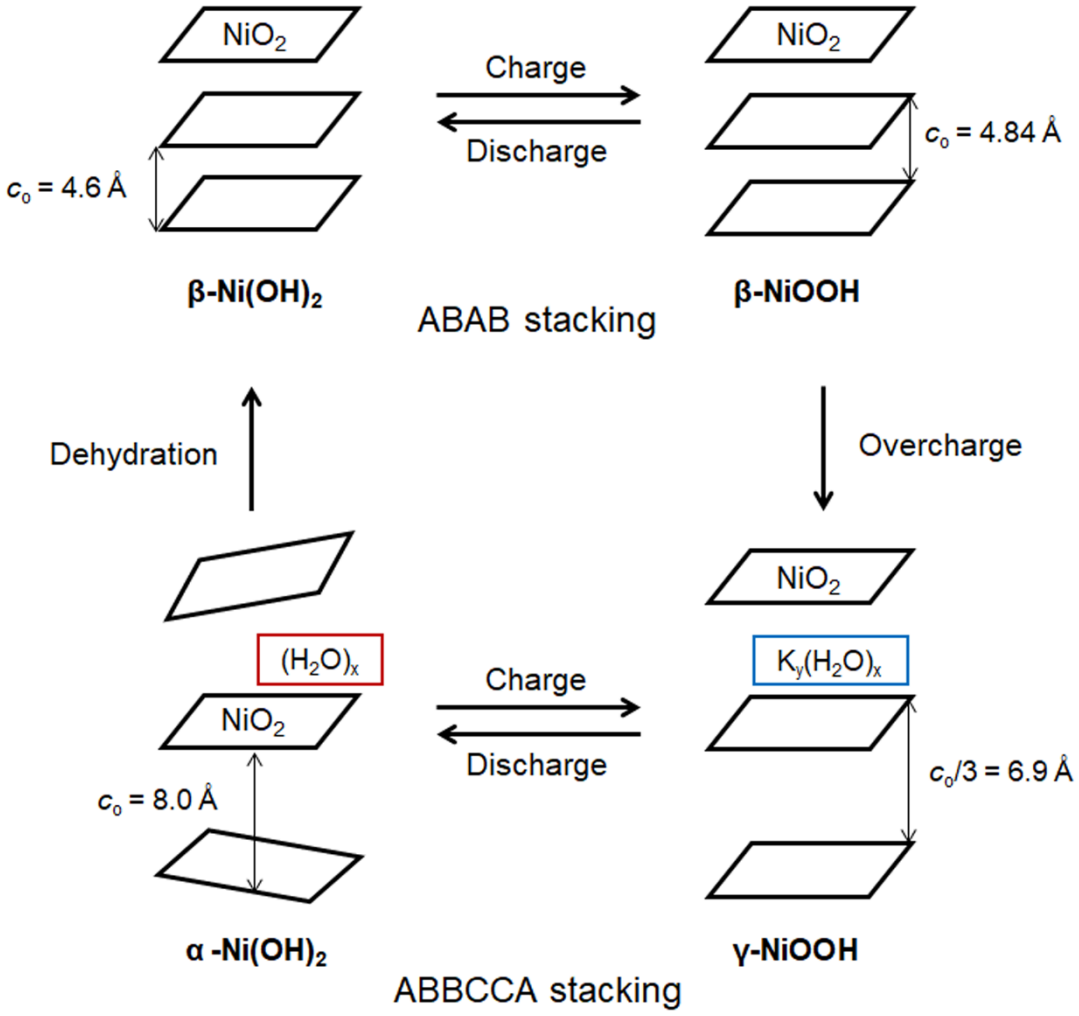

Fig. 1-1 Bode's diagram[3].

1.2 Lead Acid Battery

1.2.1 Overview of Lead Acid Battery

It has been over 150 years since lead acid battery was invented by Plante et al., and still now, it is widely utilized for the energy storage device of vehicles or back up power supply for the virtue of its low cost, high power density and safety [13,14]. About 30% of gross product of secondary battery is occupied by lead acid battery, and no-idling operation for recent automobiles enhance the importance of corrosion of current collector (CC) during the rest time. Furthermore, for the power source of photovoltaic power generation or wind power generation, the demand for lead acid battery would be increased because of its low cost.

1.2.2 Electrode Materials of Lead Acid Battery

For the electrode materials of lead acid battery, lead oxide and lead are used for cathode and anode active materials. For the practical lead acid battery, lead alloy is generally used as current collector for cathode side and about 30wt% sulfuric acid is used as electrolyte. When the battery is discharged, lead oxide and lead changes into lead sulfate. Because lead sulfate does not have the electric conductivity, crystallization of lead sulfate affects the battery performance critically, and this phenomenon is called as sulfation. Chemical reactions for lead acid battery are shown below. To prevent sulfation caused by lead sulfate, the product of discharge, to keep the state of charge in the high region is suitable for the operation of lead acid battery.

Cathode: $PbO_2 + 4H^+ + SO_4^{2-} + 2\,e^- \rightleftarrows PbSO_4 + 2H_2O$

Anode: $Pb + SO_4^{2-} \rightleftarrows PbSO_4 + 2e^-$

※ Right direction describes discharge reaction and left direction describes charge reaction.

1.2.3 Lead Dioxide

Lead dioxide has the high electric conductivity and has the two polymorphs, i.e. α-phase and β-phase [15]. The features of α-phase and β-phase are shown in Table 1-1, and the crystal structures are shown in Fig. 1-2. The crystal symmetry of α-phase is orthorhombic, while that of β-phase is tetragonal. Therefore, α-phase and β-phase show the different XRD patterns, and α-phase has the characteristic peaks in $2\theta = 28°$ and 45°. For the pH region, α-phase is stable in high pH region while β-phase is stable in low pH region. At the inside of lead acid battery, because sulfuric acid is used as electrolyte, lead dioxide should exist as β-phase which is stable in low pH condition. However, in the cathode of practical lead acid battery, α-phase and β-phase coexist in spite of the low pH condition.

Table 1-1 Characteristics of α and β phases of lead dioxides [15].

	α-phase	β-phase
Color	brown	black
Crystal system	orthorhombic	tetragonal
pH region	high	low
Resistivity (Ω・cm)	10^{-3}	4×10^{-3}
Capacity (Ah/g)	0.12	0.16

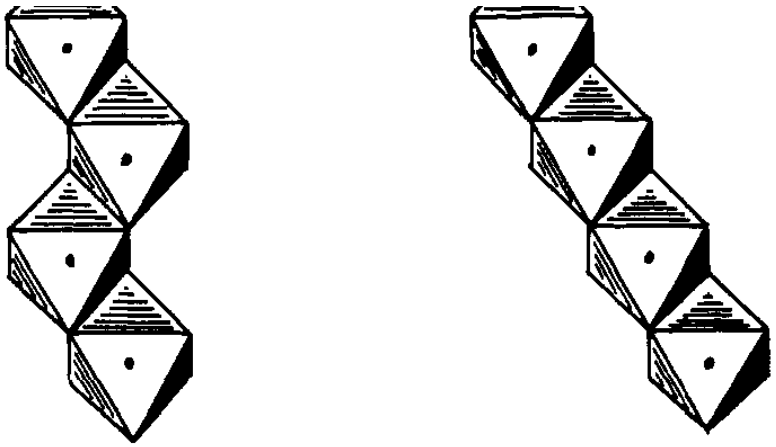

(a) (b)

Fig. 1-2 The crystal structure of (a) α-PbO_2 and (b) β-PbO_2 [15].

1.3 Local Cell Reaction

All of the materials have the different potential, and especially when the different two metals touch, current flows at the interface of two metals due to the difference of electrochemical potentials. This chemical reaction is called local cell reaction (LCR).

One practical example of LCR is galvanized iron and tinplate as shown in Fig. 1-3. For tinplate, because the surface of iron is coated by tin which has the higher potential than iron, the corrosion of iron occurs. On the other hand, for galvanized iron, because iron is coated by zinc which has the lower potential than iron, zinc is ionized and the corrosion of iron inside is prevented.

LCR occurs in the practical use of the battery. Electrode materials of practical batteries consist of some different chemicals and when the battery is not charged or discharged, LCR between the different chemicals should occur.

The studies during the rest time period of the battery seem to be quite few compared with the reports about the charge-discharge process of the battery. Therefore, in this study, LCR during the rest time period and the effect of LCR on the performance of the battery were mainly investigated.

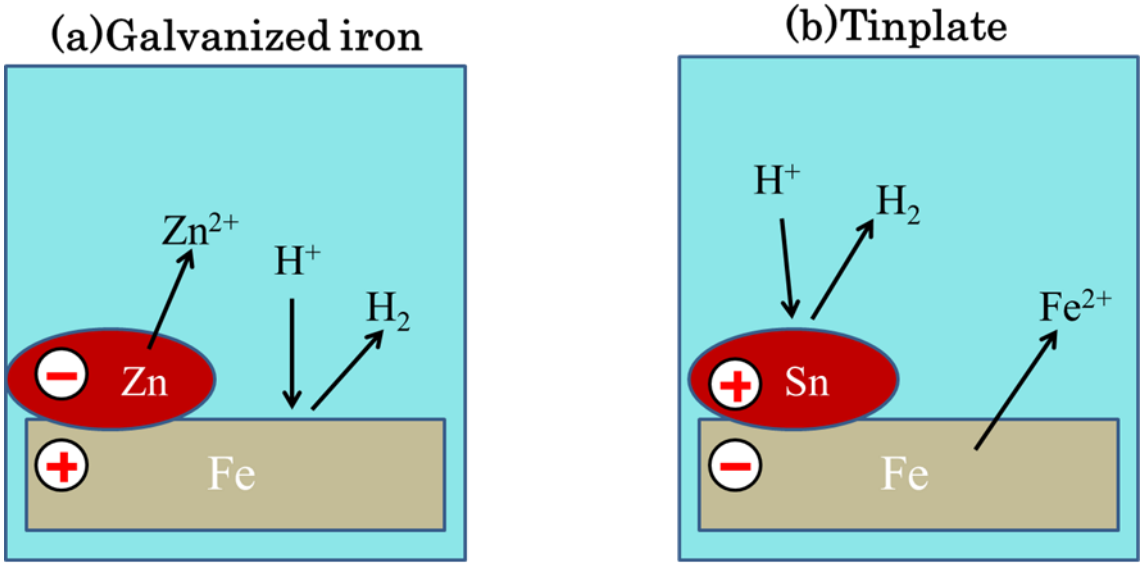

Fig. 1-3 Mechanism of local cell reaction. (a) Galvanized iron and (b) Tinplate.

References

[1] B. Mebarki, B. Draoui, L. Rahmani, B. Allaoua, Electric Automobile Ni-MH Battery Investigation in diverse situations, *Energy Procedia*, 36 (2013) 130-141. [DOI: 10.1016/j.egypro.2013.07.016]

[2] P. Oliva, J. Leonardi, J.F. Laurent, C. Delmas, J.J. Braconnier, M. Figlarz, F. Fievet, A.D. Guibert, Review of the structure and the electrochemistry of nickel hydroxides and oxy-hydroxides, *J. Power Sources*, 8 (1982) 229-255. [DOI: 10.1016/0378-7753(82)80057-8]

[3] H. Bode, K. Dehmelt, J. Witte, Zur kenntnis der nickelhydroxidelektrode - I.Über das nickel (II) – hydroxidhydrat, *Electrochim. Acta*, 11 (1966) 1079-1087. [DOI: 10.1016/0013-4686(66)80045-2]

[4] O. Glemser, J. Einerhand, Über höhere Nickelhydroxyde, Z. Anorg. *Allg. Chem*., 261 (1950) 26-42. [DOI: 10.1002/zaac.19502610103]

[5] R. Juza, W. Meyer, Über Uran-Nitrid-Chlorid, -Bromid und -Jodid, Z. Anorg. *Allg. Chem*., 366 (1969) 1-2. [DOI: 10.1002/zaac.19693660105]

[6] C. Faure, C. Delmas, P. Willmann, Preparation and characterization of cobalt-substituted α-nickel hydroxides stable in KOH medium Part I. α′-hydroxide with an ordered packing, *J. Power Sources* 35 (1991) 249-261. [DOI: 10.1016/0378-7753(91)80110-J]

[7] N. Sac-Epée, M.R. Palacin, B. Beaudoin, A. Delahaye-Vidal, T. Jamin, Y. Chabre, J.-M. Taraican, On the Origin of the Second Low-Voltage Plateau in Secondary Alkaline Batteries with Nickel Hydroxide Positive Electrodes, *J. Electrochem. Soc.* 144 (1997) 3896-3907. [DOI: 10.1149/1.1838108]

[8] C. Leger, C. Tessier, M. Menetrier, C. Denage, C. Delmas, Investigation of the Second Discharge Plateau of the β(III)- NiOOH / β(II)-$Ni(OH)_2$ System, *J. Electrochem. Soc.* 146 (1999) 924-932. [DOI: 10.1149/1.1391701]

[9] C. Tessier, L. Guerlou-Demourgues, C. Faure, M. Basterreix, G. Nabias, C. Delmas, Structural and textural evolution of zinc-substituted nickel hydroxide electrode materials upon ageing in KOH and upon redox cycling, *Solid State Ionics*, 133 (2000) 11-23. [DOI: 10.1016/S0167-2738(00)00690-1]

[10] F. Bardé, M.R. Palacin, B. Beaudoin, J.-M. Tarascon, Ozonation: A Unique Route To Prepare Nickel Oxyhydroxides. Synthesis Optimization and Reaction Mechanism Study, *Chem. Mater*. 17 (2005) 470-476. [DOI: 10.1021/cm040133+]

[11] X.-Z. Fu, Y.-J. Zhu, Q.-C. Xu, J. Li, J.-H. Pan, J.-Q. Xu, J.-D. Lin, D.-W. Liao, Nickel oxyhydroxides with various oxidation states prepared by chemical oxidation of spherical β-$Ni(OH)_2$, *Solid State Ionics*, 178 (2007) 987-993. [DOI: 10.1016/j.ssi.2007.04.011]

[12] J. Pan, J. Du, Y. Sun, P. Wan, X. Liu, Y. Yang, The change of structure and electrochemical property in the synthesis process of spherical NiOOH, *Electrochim Acta*, 54 (2009) 3812-3818. [DOI: 10.1016/j.electacta.2009.01.083]

[13] S.S. Misra, T.M. Noveske, S.L. Mraz and A.J. Williamson, *J. Power Sources*, 95 (2001) 162-173.

[DOI: 10.1016/S0378-7753(00)00616-9]

[14] T. Huang, W. Ou, B. Feng, B. Huang, M. Liu, W. Zhao and Y. Guo, *J. Power Sources*, 210

(2012) 7-14. [DOI: 10.1016/j.jpowsour.2012.02.086]

[15] K. Ji, C. Xu, H. Zhao and Z. Dai, *J. Power Sources*, 248 (2014) 307-316. [DOI: 10.1016/j.jpowsour.2013.09.112]

Chapter 2 Effect of Local Cell Reaction on the Performance of Nickel Metal-Hydride Battery

2.1 Introduction

Nickel metal-hydride battery is taking a great attention as the most practical secondary battery for the power sources of hybrid vehicles due to its relatively high discharge capacity and safety [1]. In addition, it is still useful for the back-up power sources or portable devices. However, it has been well known that nickel metal-hydride batteries reduce the capacity after the shallow charge-discharge cycles [2-4], which is sometimes referred as memory effect [5-7]. Before the development of nickel metal-hydride battery, the widely used was nickel cadmium battery, in which the battery degradation due to shallow charge-discharge cycles has also been the critical issue [8-10]. Huggins ascribed the degradation of the nickel cadmium battery to the passivation of cadmium anode [11,12]. However, even after nickel metal-hydride battery with different anode (hydrogen absorbing alloy) had been developed, such a degradation has been still reported [7,13-15]. Consequently, β-NiOOH of the common cathode material of nickel cadmium battery and nickel metal-hydride battery has been thought to be the cause of the degradation. Sato et al. ascribed the battery degradation to the formation of γ-NiOOH, which is an oxidant of β-NiOOH (Though the precise valence of nickel for β and γ phases are not defined, the valences are thought to be 2.8～3.2 for β phase and 3.6～3.67 for γ phase, respectively.) [16,17], at the interface between current collector (CC) and cathode active material (β-NiOOH) [5-7]. However, the detailed mechanism of the γ-NiOOH formation at the CC side instead of electrolyte side has not been revealed. The local cell reaction is thought to be the major factor of the transformation of β-NiOOH, since the reaction occurs between cathode active material and CC in the open circuit [18]. In the present chapter, the phase formation and the cell performance were compared by employing various metals as CC focusing on the local cell reaction between cathode active material and CC.

2.2 Experimental

2.2.1 Synthesis of Cathode Active Material

β-NiOOH of the cathode active material was synthesized by oxidizing nickel hydroxide (Aldrich Chemical Co., Inc) as the reported procedure [19]. 0.4 g of nickel hydroxide was mixed with 10 mL of distilled water to make a slurry, into which 10 mL of an aqueous solution of sodium hypochlorite was then added to oxidize nickel hydroxide. The solution was kept at 20 ℃ for 1.5 hours to proceed the reaction. The product material was thereafter separated by vacuum filtration, washed by distilled water and dried for 1 day at 40 ℃. After the processes above, black solid of β-NiOOH was obtained.

2.2.2 Charge-Discharge Cycles with Rest Time

The cathode was fabricated by mixing powder of the synthesized β-NiOOH as the active material, acetylene black as a conducting additive and PTFE as a binder at the ratio of 80:15:5 in weight. Platinum plate and Ag/AgCl electrodes were used as counter and reference electrodes, respectively. The electrolyte used was an 8 M potassium hydroxide. Three kinds of current collectors (CC) of nickel, gold and platinum meshes were employed to compare the local cell reaction with the active material. Focusing on the local cell reaction between the pure β-NiOOH and CC, zinc or cobalt hydride was not added which is used for the commercial battery to improve the battery performance. For each CC, six kinds of charge-discharge cycles below (Ex. 1, Ex. 2 (A), (B), (C), and Ex. 3 (A), (B)) were conducted.

For Ex. 1, the cell was at first discharged to the cutoff voltage of 0.19 V (vs. SHE, Standard Hydrogen Electrode), followed by charging for 6 hours to achieve the full charged state. The cell was then discharged for 50 $mAhg^{-1}$ of NiOOH, which is about a half of the cell capacity. After that, the circuit was opened for 1 day for nickel mesh and 3 days for gold and platinum meshes. This open circuit period is referred as rest time hereafter.

For Ex. 2, the cell was initially discharged to the cutoff voltage of 0.19 V (vs. SHE) and charged for 6 hours, the cycle of which has been repeated for 3 times to stabilize the cell reaction. After the cycles of stabilization process, the charge-discharge cycle tests have been carried out. Three types of potential regions as (A) 20 – 40% of the state of charge

(SOC), (B) 40 – 60% SOC and (C) 80 – 100% SOC are selected. In these charge-discharge processes, 2 hours of rest time were inserted every end of charge and discharge processes to investigate the local cell reactions occurring at the open cell circuit. Additionally, the charge-discharge cycle tests without rest time were conducted for 40 - 60%SOC region in Ex. 2(D) for the comparison with Ex. 2(B).

After the experiments of Ex. 2 (A) and (B), Ex. 3 was conducted for the degraded cells with nickel mesh CC. Full charge (6 hours of charging) and discharge (down to cut-off voltage of 0.19 V vs. SHE) were carried out for 10 times to observe the recovery of the battery.

All of the charge-discharge cycles were conducted at a current density of 30 mAg^{-1}.

2.2.3 X-ray Diffraction Measurement

After the charge-discharge experiments, Ex. 1, Ex. 2, and Ex. 3, the cathodes with CC were mounted on a X-ray diffractometer (RINT-TTR, Rigaku) and X-ray analyses were conducted. XRD patterns were collected from 10° to 70° in 2θ at a rate of 2° per minute with 0.04° step width by using CuKα radiation. The tube voltage and current were set to 30 kV and 200 mA, respectively.

2.3 Results and Discussion

Fig. 2-1 (a), (b) and (c) represent the XRD patterns after Ex. 1 for nickel mesh, gold mesh and platinum mesh CCs, respectively. For nickel CC in (a), a weak XRD peak was observed around 13° in 2θ, although such a peak was not for the case of (b) gold or (c) platinum CCs even for the longer rest time in comparison with the nickel CC. When the global circuit is opened, the possible reaction to occur is local cell reaction between the cathode active material (β-NiOOH) and CC. Considering that the employed electrolyte and β-NiOOH are common for all the experiments in Ex. 1, the reaction between the electrolyte and β-NiOOH should not be ascribed. Comparing the potential of CCs, nickel (-0.26 V vs. SHE) has the lower potential than that of β-NiOOH (0.48 V vs. SHE) [20-23], while gold (1.50 V vs. SHE) or platinum CC (1.12 V vs. SHE) has the higher ones. Therefore, β-NiOOH and nickel CC should act as cathode and anode, respectively during

rest time by local cell reaction. Although γ-NiOOH shows diffraction peak around 2θ = 13° for CuK_α radiation [5,19], it should not be formed by the local cell reaction since the potential stable for γ-NiOOH is higher than that for β-NiOOH. Assuming that γ-NiOOH can be derived from β-phase by the different stacking of the NiO_2 layers or intercalation according to the Bode's diagram (Fig. 2-2), similar derivatives can be expected [24-31]. To distinguish from the higher potential phase γ-NiOOH, this reduced product obtained by above experiment is referred as γ'-NiOOH hereafter. The XRD peak around 13° is *d* = 7 Å, which corresponds to 001 lattice spacing of γ-polymorphs [32-35]. γ'-NiOOH is thought to have the intermediate structure of γ-NiOOH and α-$Ni(OH)_2$ in the Bode's diagram as shown in Fig. 2-2. When β-NiOOH is overcharged at the high potential around 0.5V (vs. SHE), potassium ion and water molecule intercalate between the NiO_2 layers to transform into γ-NiOOH. For the structure of α-$Ni(OH)_2$, only water molecule intercalates [36]. The XRD peak of γ'-NiOOH differs from that of α-$Ni(OH)_2$ and the rest potential is lower than 0.5V (vs. SHE) [37]. Therefore, it is considered that γ'-NiOOH has the intermediate potential between γ-NiOOH and α-$Ni(OH)_2$, and that γ'-NiOOH is formed when nickel ion is intercalated to reduce β-NiOOH at the lower potential than 0.5 V due to the local cell reaction.

It is widely known that battery degradation would occur only when the battery is left open circuit after charging or discharging to the intermediate SOC regions [5-7]. Since the battery is discharged about 50%SOC in above Ex. 1, formation of γ'-NiOOH is thought to cause the battery degradation. To confirm the relationship between the battery degeneration and formation of γ'-NiOOH, and to clarify the SOC regions of γ'-NiOOH formation, the shallow charge-discharge experiments were conducted at restricted SOC regions in Ex. 2.

As the fundamental electrochemical property, full discharge curves after charge of 6 hours to 10 cycles are shown in Fig. 2-3. For the cycleability of $Ni(OH)_2$, stable charge and discharge are repeated for all CCs after 3 cycles. On the other hand, for the capacity of the cell, when the gold or platinum mesh are used, the discharge capacity and the potential are both higher than the case of nickel mesh. High potential and conductivity of gold or platinum mesh is assumed to cause these results. Considering the results, 3 cycles

are enough to stabilize the cell and 3 cycles of full charge and discharge were conducted for the stabilization process in Ex.2 and Ex.3.

Discharge curves during charge-discharge cycles with rest time and XRD patterns for Ex. 2 (A) (20 – 40%SOC region) are shown in Fig. 2-4 and Fig. 2-5, respectively. Only for nickel CC, the cell degradation occurs after 40 cycles and the small characteristic diffraction peak of γ'-NiOOH at 13° in 2θ was detected after the cycle test. On the other hand, for gold or platinum CCs, no degradation can be seen after 50 cycles and any trace of diffraction peak around 13° is not detected. Even for 40 – 60% SOC region, which corresponds to Ex. 2 (B), only the battery using nickel CC degenerate after 40 cycles, on which XRD peak of γ'-NiOOH has been detected as Figs. 2-6 and 2-7. Accordingly, only when the nickel CC is employed, battery degradation and formation of γ'-NiOOH are observed. On the other hand, charging and discharging at relatively higher SOC region between 80 – 100% which corresponds to Ex. 2 (C), such a battery degradation does not occur up to 50 cycles and no XRD peak of γ'-NiOOH is detected, which are shown in Figs. 2-8 and 2-9. Therefore, battery degradation due to the shallow charge and discharge in the SOC region of 20 - 60% is closely related to the formation of γ'-NiOOH, which occurs only for nickel CC.

To prove the γ'-NiOOH phase grows during the rest time, the similar experiment in the SOC region of 40 – 60% are conducted without rest time in Ex. 2 (D). The results are represented in Figs. 2-10 and 2-11. Even for nickel CC, battery degradation did not occur even after the 100 cycles of charge discharge process, and diffraction peaks of γ'-NiOOH phase did not appear. This indicates that γ'-NiOOH phase grows at the rest time. Considering the results of Ex.1 and Ex.2, it is clarified that γ'-NiOOH forms during the rest time, and is not the oxidant of β-NiOOH but the reductant because the reduction of β-NiOOH occurs in the local cell reaction.

It is assumed that γ'-NiOOH would be re-oxidized to transform into β-form at higher potential region. Ex.3 was finally conducted to confirm whether γ'-NiOOH disappears by the full charge and discharge of the cell after the degradation due to the charge-discharge cycle test in the region of SOC 40-60% and 20-40%. Fig. 2-12 shows the XRD pattern after the full charge-discharge cycles in Ex. 3. The XRD peak of γ'-NiOOH was not

detected for both Ex. 3 (A) (SOC 40-60% region) and Ex. 3 (B) (SOC 20-40% region). It is considered that γ'-NiOOH disappeared by the full charge of the cell. Fig. 2-13 shows the discharge curves for the full charge-discharge cycles. As the full charge process is repeated, the capacity of the cell was regained.

Considering the results in this chapter, the mechanism of the battery degradation due to the shallow charge-discharge (memory effect) is thought to be the formation of the reductant of β-NiOOH which occurs by the local cell reaction at the SOC region of 20 - 60%. To prevent the local cell reaction, although the employment of gold or platinum CC is not appropriate for the practical use, alternation to other higher potential material for CC, alloying of nickel, or surface coating of CC are supposed to be effective.

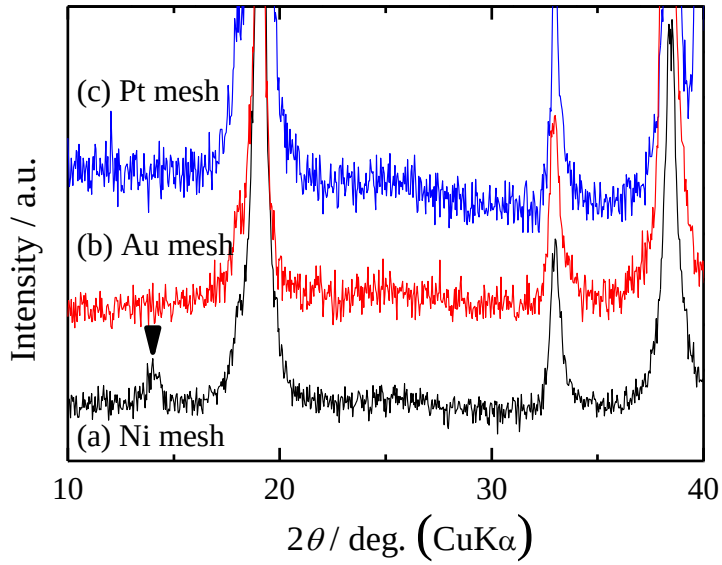

Fig. 2-1 X-ray diffraction patterns of cathode surface after the shallow discharge for Ex.1. (a), (b) and (c) show the results for nickel mesh, gold mesh and platinum mesh CCs, respectively.

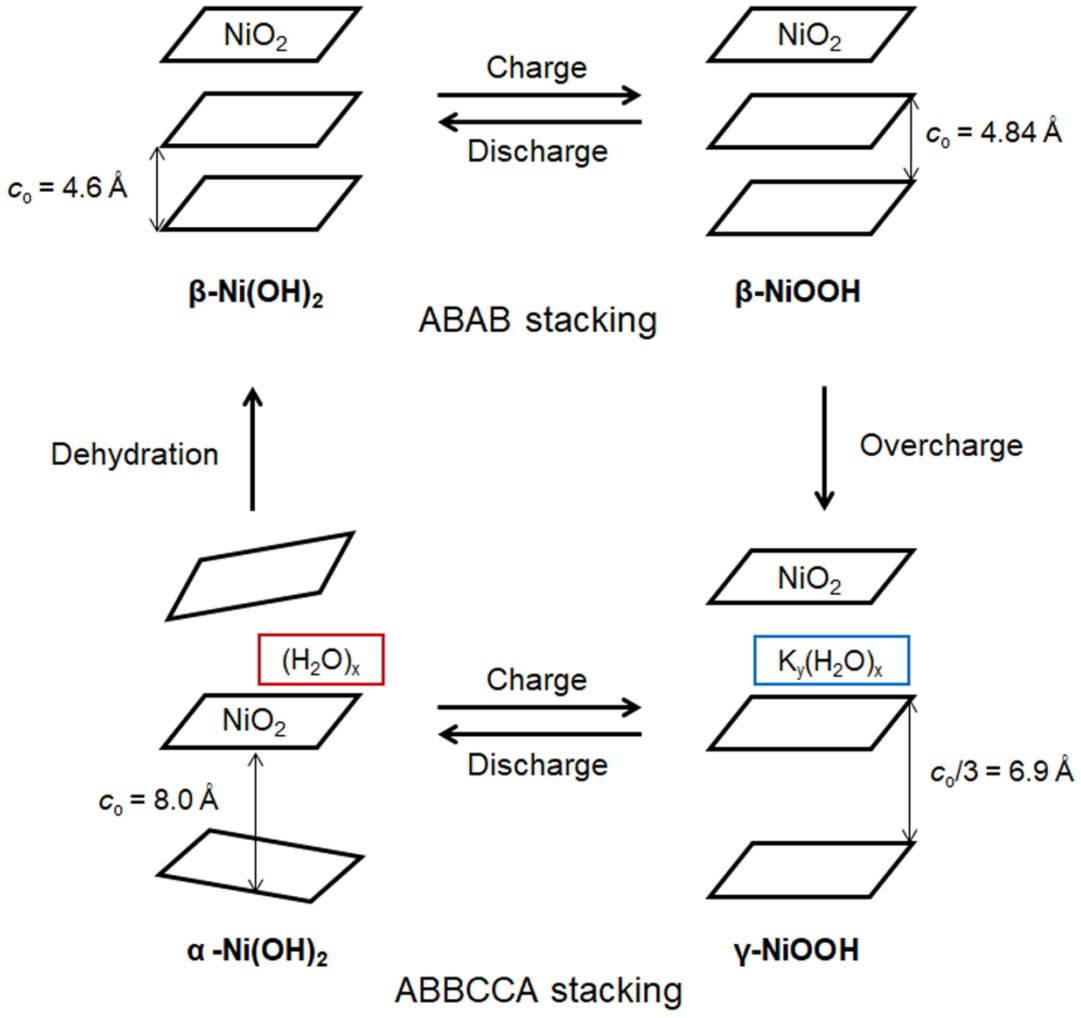

Fig. 2-2 Bode's diagram for the structures of α-$Ni(OH)_2$, β-$Ni(OH)_2$, β-NiOOH and γ-NiOOH, respectively [17].

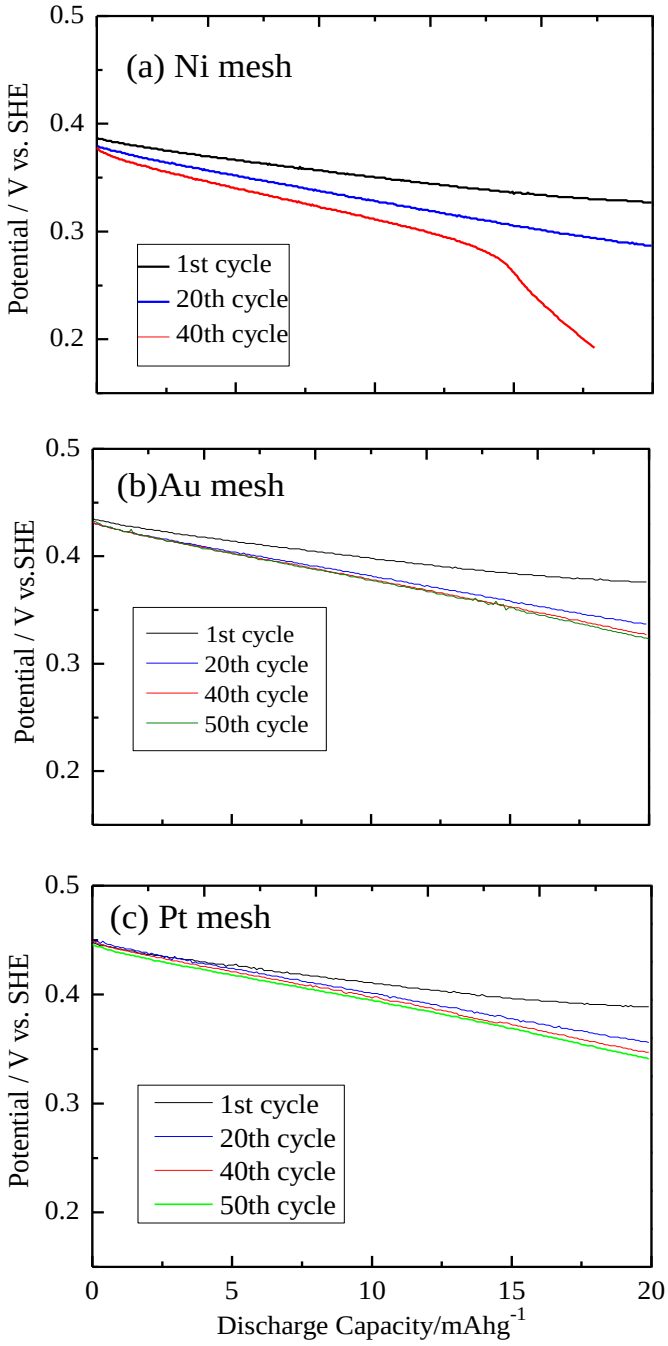

Fig. 2-3 Discharge curves for Ex.2(A) of 20 – 40 % of SOC region during the charge-discharge cycles with rest period. (a), (b) and (c) represent the results for nickel mesh, gold mesh and platinum mesh CCs, respectively.

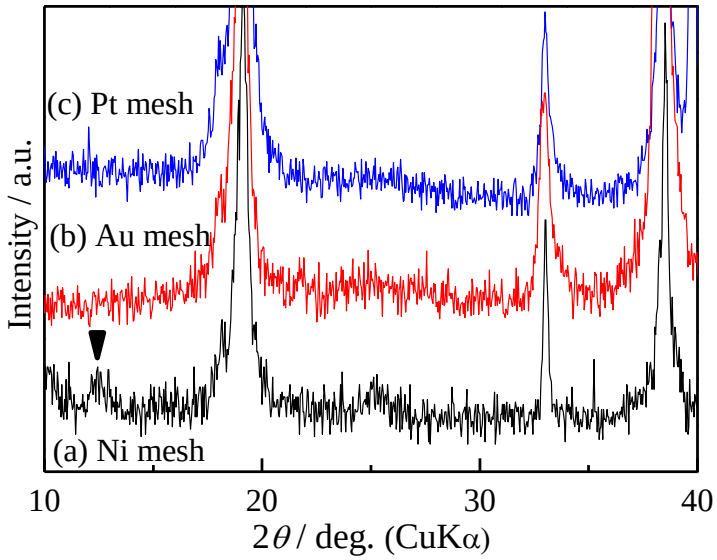

Fig. 2-4 X-ray diffraction patterns of cathode surface after the shallow discharge for Ex.2(A) of 20 – 40 % SOC region. (a), (b) and (c) show the results for nickel mesh, gold mesh and platinum mesh CCs, respectively.

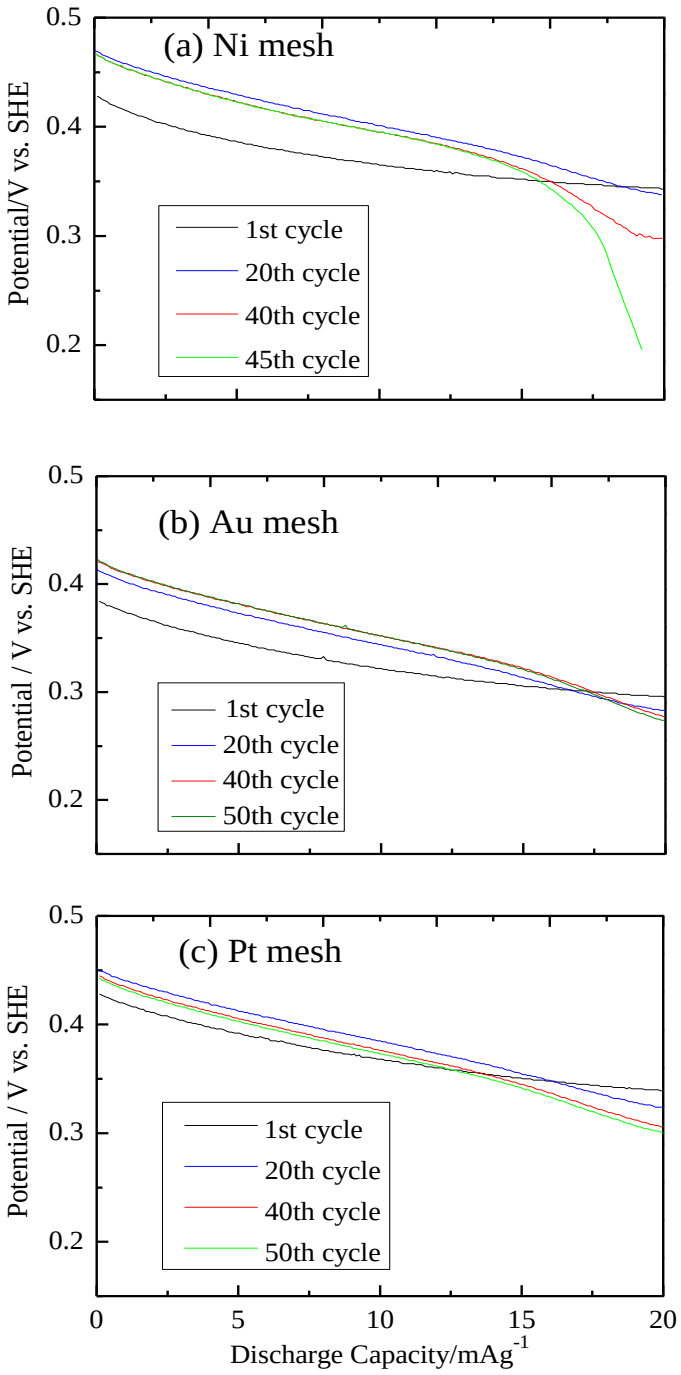

Fig. 2-5 Discharge curves for Ex.2(B) of 40 – 60 % of SOC region during the charge-discharge cycles with rest time. (a), (b) and (c) represent the results for nickel mesh, gold mesh and platinum mesh CCs, respectively.

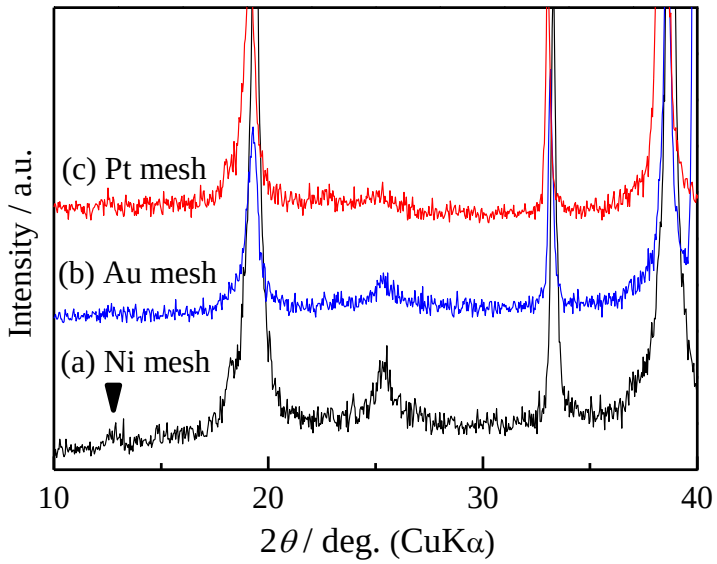

Fig. 2-6 X-ray diffraction patterns of cathode surface after the shallow discharge for Ex.2(B) of 40 – 60 % SOC region. (a), (b) and (c) show the results for nickel mesh, gold mesh and platinum mesh CCs, respectively.

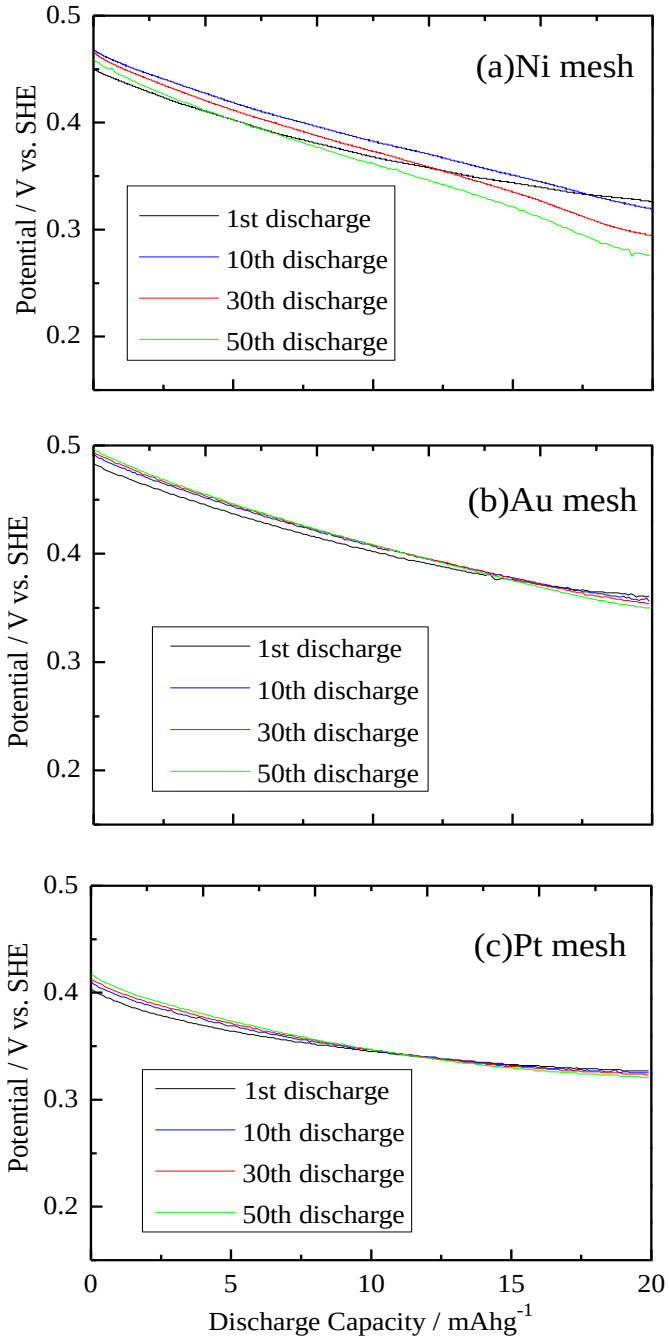

Fig. 2-7 Discharge curves for Ex.2(C) of 80 – 100 % of SOC region during the charge-discharge cycles with rest time. (a), (b) and (c) represent the results for nickel mesh, gold mesh and platinum mesh CCs, respectively.

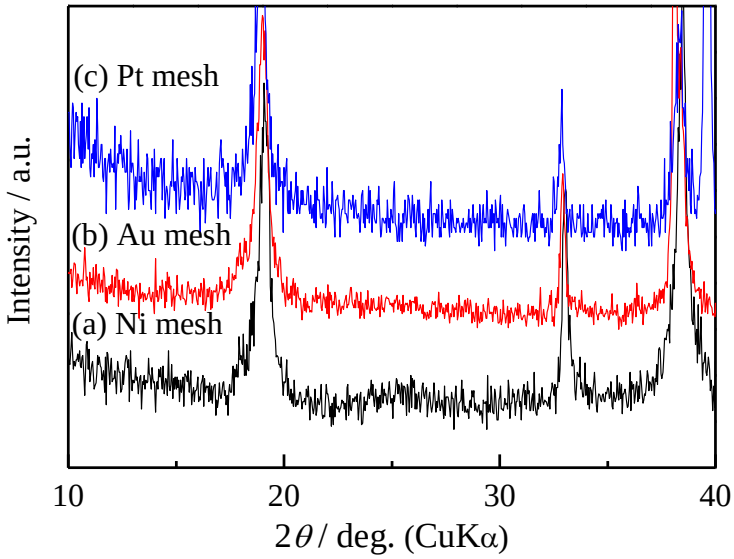

Fig. 2-8 X-ray diffraction patterns of cathode surface after the shallow discharge for Ex.2(C) of 80 – 100 % SOC region. (a), (b) and (c) show the results for nickel mesh, gold mesh and platinum mesh CCs, respectively.

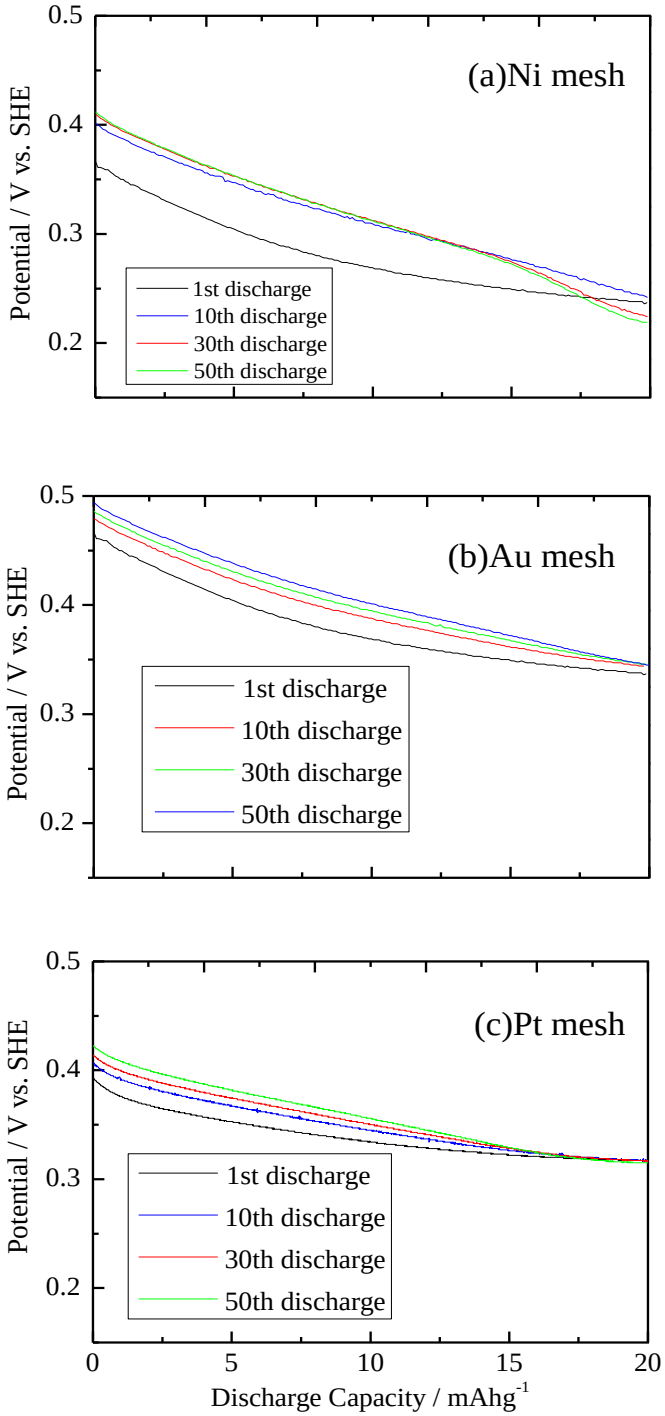

Fig. 2-9 Discharge curves for Ex.2(D) of 40 – 60 % of SOC region during the charge-discharge cycles without rest time. (a), (b) and (c) represent the results for nickel mesh, gold mesh and platinum mesh CCs, respectively.

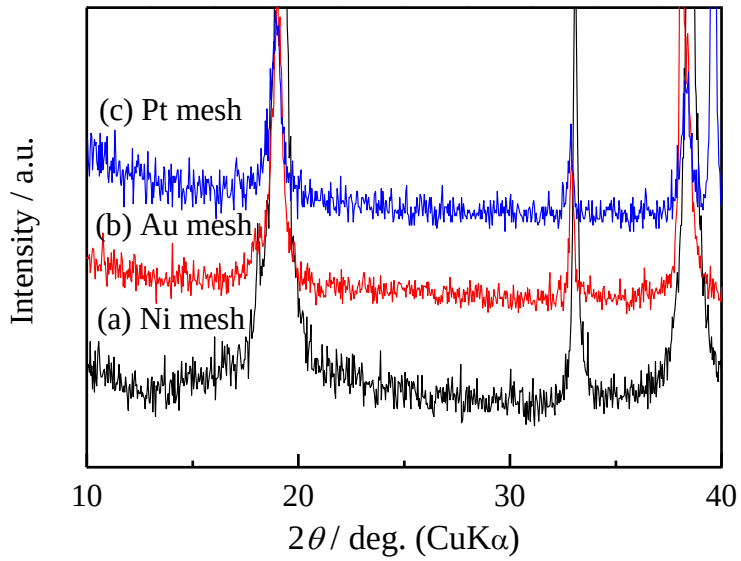

Fig. 2-10 X-ray diffraction patterns of cathode surface after the shallow discharge for Ex.2(D) of 40 – 60 % SOC region. (a), (b) and (c) show the results for nickel mesh, gold mesh and platinum mesh CCs, respectively.

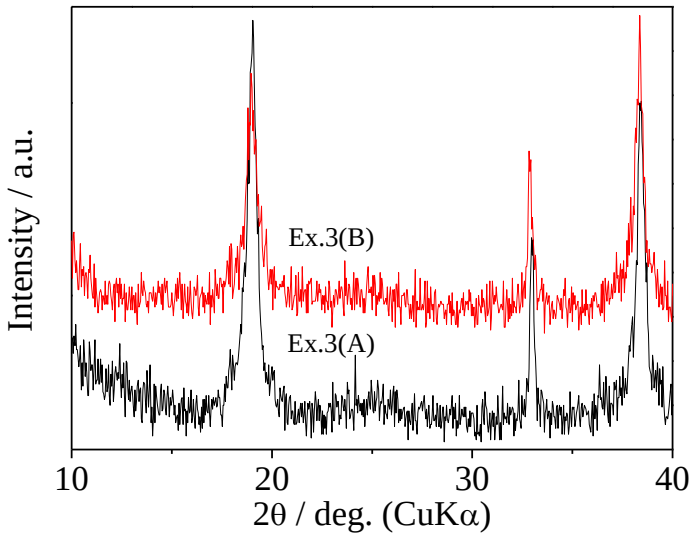

Fig. 2-11 X-ray diffraction patterns of cathode surface after the deep discharge for Ex.3(A) of 40 – 60 % SOC region and Ex.3(B) of 20 – 40 % SOC region for nickel mesh CC.

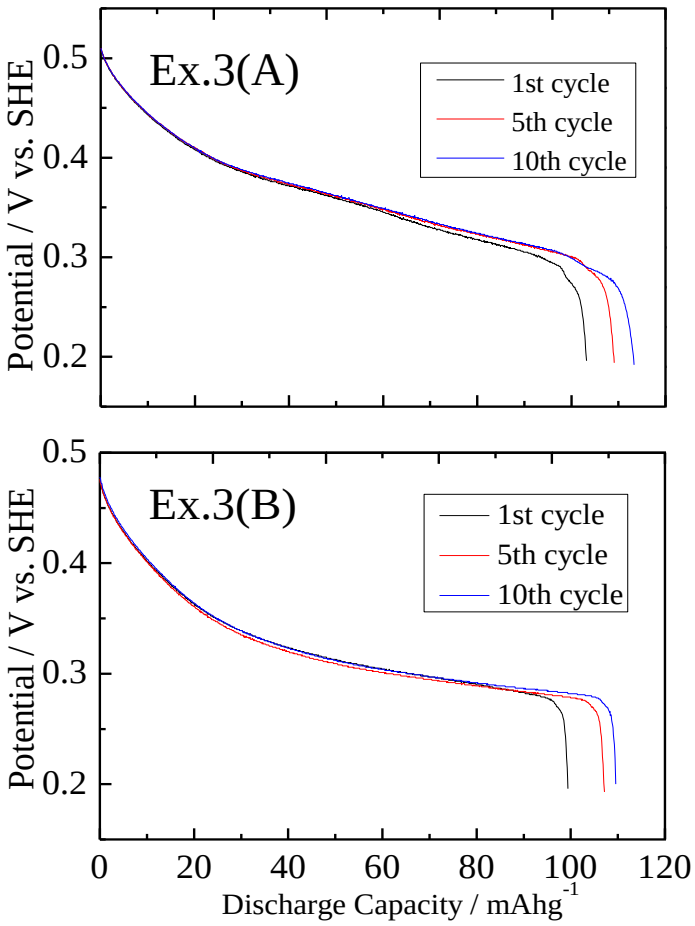

Fig. 2-12 Discharge curves for the full charge-discharge cycles in Ex.3(A) of 40 – 60 % of SOC region and Ex.3(B) of 20 – 40 % of SOC region for nickel mesh CC.

2.4 Conclusion

In this chapter, the local cell reaction between the cathode active material and CC was investigated. When CC with lower potential than β-NiOOH is used, the degradation of the cell capacity and XRD peak around 13° were observed after the shallow charge-discharge experiment with the rest time. On the contrary, when CC with higher potential than β-NiOOH is used, the degradation of the battery and XRD peak around 13° were not observed. This peak indicates the reduction of β-NiOOH to γ'-NiOOH since the performance of the battery was regained after the full charge (oxidation process) of the cell. Consequently, higher potential materials for CC would work to prevent the formation of γ'-NiOOH and the degradation of the battery. It is concluded that β-NiOOH is reduced to γ'-NiOOH to degrade the performance of the battery due to the local cell reaction between CC and the cathode active material.

References

[1] B. Mebarki, B. Draoui, L. Rahmani and B. Allaoua, *Energy Procedia*, 36 (2013) 130-141. [DOI: 10.1016/j.egypro.2013.07.016]

[2] F. Fourgeot, S. Deabate, F. Henn and M. Costa, *Ionics*, 6 (2000) 364-368.

[DOI: 10.1007/BF02374154]

[3] S. Deabate, F. Fourgeot and F. Henn, *Ionics*, 6 (2000) 415-427.

[DOI: 10.1007/BF02374162]

[4] F. Barde, M.R. Palacin, Y. Chabre, O. Isnard and J.M. Tarascon, *Chem. Mater*. 16 (2004) 3936-3948. [DOI: 10.1021/cm0401286]

[5] Y. Sato, S. Takeuchi and K. Kobayakawa, *J. Power Sources*, 93 (2001) 20-24.

[DOI: 10.1016/S0378-7753(00)00506-1]

[6] Y. Sato, K. Ito, T. Arakawa and K. Kobayakawa, *J. Electrochem. Soc*., 143 (1996) L225-L228. [DOI: 10.1149/1.1837152]

[7] M. Morishita, Y. Shimizu, K. Kobayakawa and Y. Sato, *Electrochim Acta*, 53 (2008) 6651-6656. [DOI: 10.1016/j.electacta.2008.04.066]

[8] E. Ahlberg, U. Palmqvist, N. Simica and R. Sjovall, *J. Power Sources*, 85 (2000) 245-253. [DOI: 10.1016/S0378-7753(99)00340-7]

[9] R. Barnard, G.T. Crickmore, J.A. Lee and F.L. Tye, *J. Appl. Electrochem*. 10 (1980) 61-70. [DOI: 10.1007/BF00937339]

[10] N.S. Epee, M.R. Palacin, A. D. Vidal, Y. Chabre and J.-M. Z. Tarascon, *J. Electrochem. Soc*. 145 (1998) 1434-1441. [DOI: 10.1149/1.1838501]

[11] R. A. Huggins, *Solid State Ionics*, 177 (2006) 2643-2646.

[DOI: 10.1016/j.ssi.2006.03.005]

[12] R. A. Huggins, *J. Power Source*, 165 (2007) 640-645.

[DOI: 10.1016/j.jpowsour.2006.10.031]

[13] B. Klapste, K. Mickja, J. Mrha and J. Vondrak, *J. Power Sources*, 8 (1982) 351-357. [DOI: 10.1016/0378-7753(82)80036-0]

[14] H.S. Lim and S.A. Verzwyvelt, *J. Power Sources*, 22 (1988) 213-220.

[DOI: 10.1016/0378-7753(88)80016-8]

[15] A.H. Zimmerman and P.K. Effa, *J. Electrochem. Soc*., 131 (1984) 709-713.

[DOI: 10.1149/1.2115677]

[16] P. Oliva, J. Leonardi, J.F. Laurent, C. Delmas, J.J. Braconnier, M. Figlarz, F. Fievet and A.D. Guibert, *J. Power Sources*, 8 (1982) 229-255. [DOI: 10.1016/0378-7753(82)80057-8]

[17] H. Bode, K. Dehmelt and J. Witte, *Electrochim. Acta*, 11 (1966) 1079-1087.

[DOI: 10.1016/0013-4686(66)80045-2]

[18] T. Yao, T. Iwai and H. Tagashira, PCT patent (2013), PCT /JP2013/ 74165.

[19] J. Pan, J. Du, Y. Sun, P. Wan, X. Liu and Y. Yang, *Electrochim Acta*, 54 (2009) 3812-3818. [DOI: 10.1016/j.electacta.2009.01.083]

[20] S.Deabate, F. Fourgeot and F. Henn, *Ionics*, 5 (1999) 371-384.

[DOI: 10.1007/BF02376001]

[21] S.Deabate, F. Fourgeot and F. Henn, *J. Power Sources*, 87 (2000) 125-136.

[DOI: 10.1016/S0378-7753(99)00437-1]

[22] S. Deabate and F. Henn, *J. Electrochem. Soc*., 150 (2003) J23-J31.

[DOI: 10.1149/1.1573203]

[23] S. Deabate and F. Henn, *Electrochim. Acta*, 50 (2005) 2823-2835.

[DOI: 10.1016/j.electacta.2004.11.030]

[24] O. Glemser and J. Einerhand, *Z. Anor. Allg. Chem*., 261 (1950) 26-42.

[DOI: 10.1002/zaac.19502610103]

[25] R. Juza, W. Meyer, Über Uran-Nitrid-Chlorid, Bromid-und-Jodid and Z. Anorg. *Allg. Chem*., 366 (1969) 1-2. [DOI: 10.1002/zaac.19693660105]

[26] C. Faure, C. Delmas and P. Willmann, *J. Power Sources* 35 (1991) 249-261.

[DOI: 10.1016/0378-7753(91)80110-J]

[27] N. Sac-Epée, M.R. Palacin, B. Beaudoin, A. Delahaye-Vidal, T. Jamin, Y. Chabre and J.-M. Taraican, *J. Electrochem. Soc*. 144 (1997) 3896-3907. [DOI: 10.1149/1.1838108]

[28] C. Leger, C. Tessier, M. Menetrier, C. Denage and C. Delmas, *J. Electrochem. Soc*. 146 (1999) 924-932. [DOI: 10.1149/1.1391701]

[29] C. Tessier, L. Guerlou-Demourgues, C. Faure, M. Basterreix, G. Nabias and C. Delmas, *Solid State Ionics*, 133 (2000) 11-23. [DOI: 10.1016/S0167-2738(00)00690-1]

[30] F. Bardé, M.R. Palacin, B. Beaudoin and J.-M. Tarascon, *Chem. Mater*. 17 (2005) 470-476. [DOI: 10.1021/cm040133+]

[31] X.-Z. Fu, Y.-J. Zhu, Q.-C. Xu, J. Li, J.-H. Pan, J.-Q. Xu, J.-D. Lin and D.-W. Liao, *Solid State Ionics*, 178 (2007) 987-993. [DOI: 10.1016/j.ssi.2007.04.011]

[32] D.M. MacArthur, *J. Electrochem. Soc*., 117 (1970) 422-426. [DOI: 10.1149/1.2407535]

[33] J.W. Weidner and P. Timmerman, *J. Electrochem. Soc*., 141 (1994) 346-351.

[DOI: 10.1149/1.2054729]

[34] B. Paxton and J. Newman, *J. Electrochem. Soc*., 143 (1996) 1287-1292.

[DOI: 10.1149/1.1836631]

[35] S. Motupally, C.C. Streinz and J.W. Weidner, *J. Electrochem. Soc*., 145 (1998) 29-34. [DOI: 10.1149/1.1838205]

[36] L. Liu, Z. Zhou and C. Peng, *Electrochim. Acta*, 54 (2008) 434-441.

[DOI: 10.1016/j.electacta.2008.07.055]

[37] J.J. Braconnier, C. Delmas, C. Fouassier, M. Figlarz, B. Beaudouin and P. Hagenmuller, *Rev. Chim. Miner*., 21 (1984) 496-508. [DOI: 10.1002/chin.198508039]

Chapter3 Effect of Local Cell Reaction on the Performance of Lead Acid Battery

3.1 Introduction

In the long history of study of lead acid battery over 100 years, for the improvement of the performance of lead acid battery, the development of current collector (CC) with high corrosion-resistance was investigated to avoid the corrosion of CC which considerably shorten the battery life [1]. To prevent the anodic oxidation of CCs caused by the overcharge of the battery, various alloys, e.g. Pb-Ca-Sn or Pb-Sb-Sn systems, was developed for the CC of the cathode [2]. Furthermore, as it appears to be difficult to prevent the corrosion completely as far as lead was used [2,3], lead-free CC such as Ti-SnO_2 was explored. As for the corrosion mechanism of CC, while several studies were reported on the corrosion process occurring during charge-discharge cycles [4-6] or on the self-discharge and passivation phenomena [7,8], relatively few researches focused on the local cell reaction during the rest time. When the circuit is open, local cell reaction (LCR) between the electrode material and the CC will occur. It is newly found that LCR plays an important role on the performance of the battery [9]. In this chapter, the effect of LCR on the cathode material of lead acid battery was investigated. Cathode active material for lead acid battery is β-PbO_2, which has higher potential than lead. When lead is used as CC, it is considered that β-PbO_2 works as anode and that the lead works as cathode due to LCR at the rest time. On the other hand, when a material which has higher potential than β-PbO_2 is used as CC, the polarity will be reversed, i.e. β-PbO_2 works as cathode and that CC works as anode. Gold and platinum meshes are presently employed for higher potential CCs than β-PbO_2. The discharge capacity and the resultant phase of β-PbO_2 were compared by employing lead, gold and platinum as CC materials, and investigated the cell degradation mechanisms of lead acid battery during the rest time.

3.2 Experimental

3.2.1 Sample Preparation

Two-electrode glass cell was constructed for charge-discharge experiments as shown in Fig.3-1. The cathode paste has been prepared by mixing the purchased β-PbO_2 powder (A Johnson Matthey) as an active material, acetylene black as a conducting additive and PTFE as a binder at the ratio of 80:15:5 in weight. Cathode was then fabricated by pressing the paste on a current collector (CC). The typical electrode area is 3 ~ 4 cm^2. Three kinds of CCs which are stable in the 30 wt% sulfuric acid were employed, i.e. lead plate, gold mesh and platinum mesh. Lead plate and 30 wt% sulfuric acid (H_2SO_4) were employed as counter electrode and electrolyte, respectively.

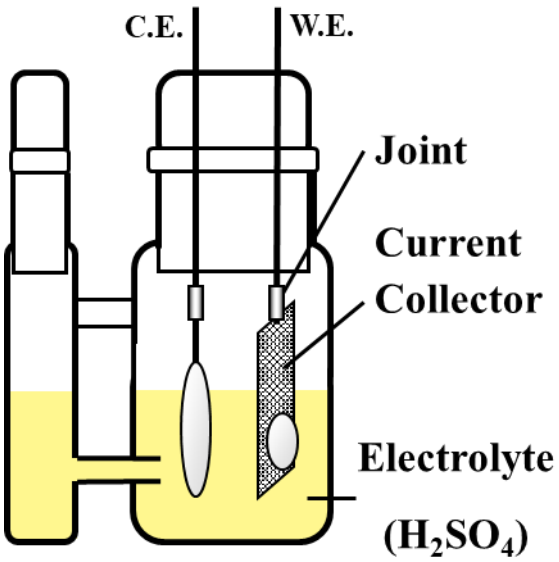

Fig.3-1 Two electrodes glass cell.

3.2.2 X-ray Diffraction Measurement

To investigate the products by LCR, X-ray diffraction measurements were carried out after charge-discharge tests. Cathode was mounted on a diffractometer (RINT-TTR, Rigaku) and subjected to CuKα radiation (30 kV, 200 mA). Diffracted X-ray was collected in the 2θ range from 20° to 90° with 0.01° step for 10 second dwell time in each step.

3.2.3 Electrochemical Cycle Test

At first, the cell was discharged at 9 mAg^{-1} for 30 minutes and charged at 180 mAg^{-1} for 20 minutes, which was cycled for 20 times to make the charge-discharge reaction stable. The cut off voltages is selected as 0 V when the cell is discharged. The process is referred as the stabilization process hereafter. Then the following experiments are conducted, Ex.1 and Ex.2. For Ex.1, after the stabilization of the cell reaction, the cell was deeply discharged down to 0 V at 9 mAg^{-1} and opened the circuit for various rest time periods from 0 hour to 48 hours. For Ex.2, after the rest of 24 hours of Ex.1, the cell was once charged at 180 mAg^{-1} for 1 hour, thereafter discharged at 9 mAg^{-1} for 30 minutes and charged again at 180 mAg^{-1} for 20 minutes, which were cycled for 20 times to study the effect of products on the cell performance.

3.3 Results and Discussion

The results of Ex.1 including charge-discharge curves and the XRD measurements are represented from Fig.3-2 to Fig.3-5. In Fig.3-2, charge-discharge curves for the stabilization process are shown for (a) lead plate, (b) gold mesh and (c) platinum mesh CCs. After the first 10 cycles, charge-discharge curves became stable between 1.0 and 3.0 V for all cells. For the charge-discharge curves, any significant difference was not detected among the materials of CC. Fig.3-3 shows the XRD patterns of the cathode after the stabilization process for (a) lead plate, (b) gold mesh and (c) platinum mesh CCs below 35° in 2θ, since any apparent difference is not observed for higher 2θ region. For XRD patterns after the stabilization, the difference due to the CC was not detected. Fig.3-4 shows the charge-discharge curves after the stabilization process and the deep discharge down to 0 V for (a) lead plate, (b) gold mesh and (c) platinum mesh CCs, and Fig.3-5 shows the XRD patterns in the open circuit after the deep discharge. The rest time periods were selected as (i) 0 hour, (ii) 6 hours, and (iii) 48 hours. The difference of charge-discharge curves was not detected for all CCs. However, for the lead plate CC as shown in Fig.3-5(a), a diffraction peak around 28° in 2θ identified as α-PbO_2 [10] is not detected for (i) but is for (ii) and (iii). Therefore, α-PbO_2 should grow in the rest time period. Fig.3-

5 (b) and (c) represent the results for gold mesh and platinum mesh CCs, respectively, where the peak around 28° of α-PbO_2 is not detected even after 48 hours of the rest period for both CCs. Among the two polymorphs of PbO_2, it has been reported that α-PbO_2 is a reductant of β-PbO_2 [1]. Creation of α-PbO_2 has been thought to be through the anodic oxidation of lead oxide in the cathode of lead acid battery as the following model [4]. Lead sulfate crystals grow at first by the reaction between the cathode active material and sulfuric acid electrolyte to cover the surface of the cathode, and consequently, pH is increased to form lead oxide in the region between lead sulfate and the CC. The formed lead oxide is then oxidized into α-PbO_2 by the oxygen in sulfuric acid at the charge process of the battery. However, anodic oxidation should not occur to form α-PbO_2 during the rest time period, since the current cannot flow in the condition of open circuit. Since the diffraction peak of α-PbO_2 grows larger with increasing the rest time period as observed in Fig.3-5 (a), α-PbO_2 formation should occur due to LCR. Moreover, as observed in Fig.3-5 (b) and (c), α-PbO_2 does not form for noble CC materials, which also supports the LCR model. Namely, only when the lower potential CCs such as lead plate is adopted, the reduction of β-PbO_2 occurs due to LCR during rest time period.

To investigate the effect of α-PbO_2 formation on the performance of the lead acid battery, further charge-discharge cycles were conducted after the rest time periods in Ex.2. Fig.3-6 (a), (b), and (c) shows the charge-discharge curves after 48 hours of rest using lead plate, gold mesh and platinum mesh CCs, respectively. Since the cell with lead CC (a) has almost lost the charge-discharge ability after the rest time, 20 times of charge-discharge cycle have accomplished within 80 seconds due to the cut-off voltage. On the other hand, for gold or platinum mesh CC, the cell still shows the charge and discharge ability after 48 hours of the rest time period as (b) or (c). Fig.3-7 shows the XRD patterns of cathode after the charge-discharge cycles of Fig. 3-6. Diffraction peak of α-PbO_2 is detected only for (a). Considering that α-PbO_2 has the electronic conductivity, the formation of α-PbO_2 is not likely to become the direct reason of battery degradation. Surface corrosion of CC to form α-PbO_2 might induce the cell degradation.

Summarizing the present chapter, it is found that α-PbO_2 formation due to LCR and the consequent battery degradation occur for employing lead plate CC which has the lower

potential than β-PbO_2. For further understanding of the reaction during the rest time period, the oxidation condition of lead at the interface between the cathode active material and CC was investigated with XPS analysis and the impedance measurements before and after the battery degradation were conducted. The results are shown in the next chapter.

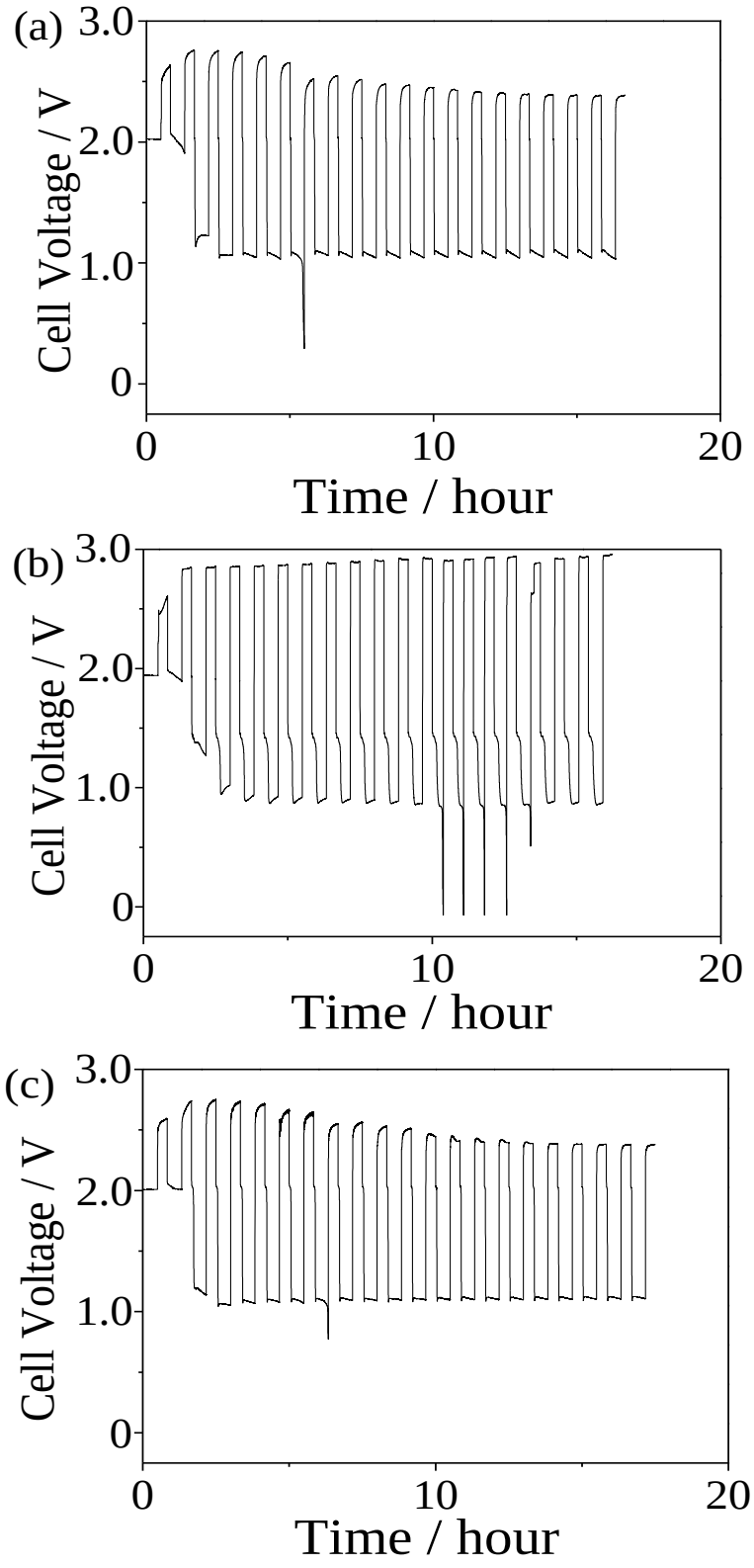

Fig.3-2 Charge-discharge curves of the lead acid battery for the stabilization process using (a) lead plate, (b) gold mesh and (c) platinum mesh as CCs.

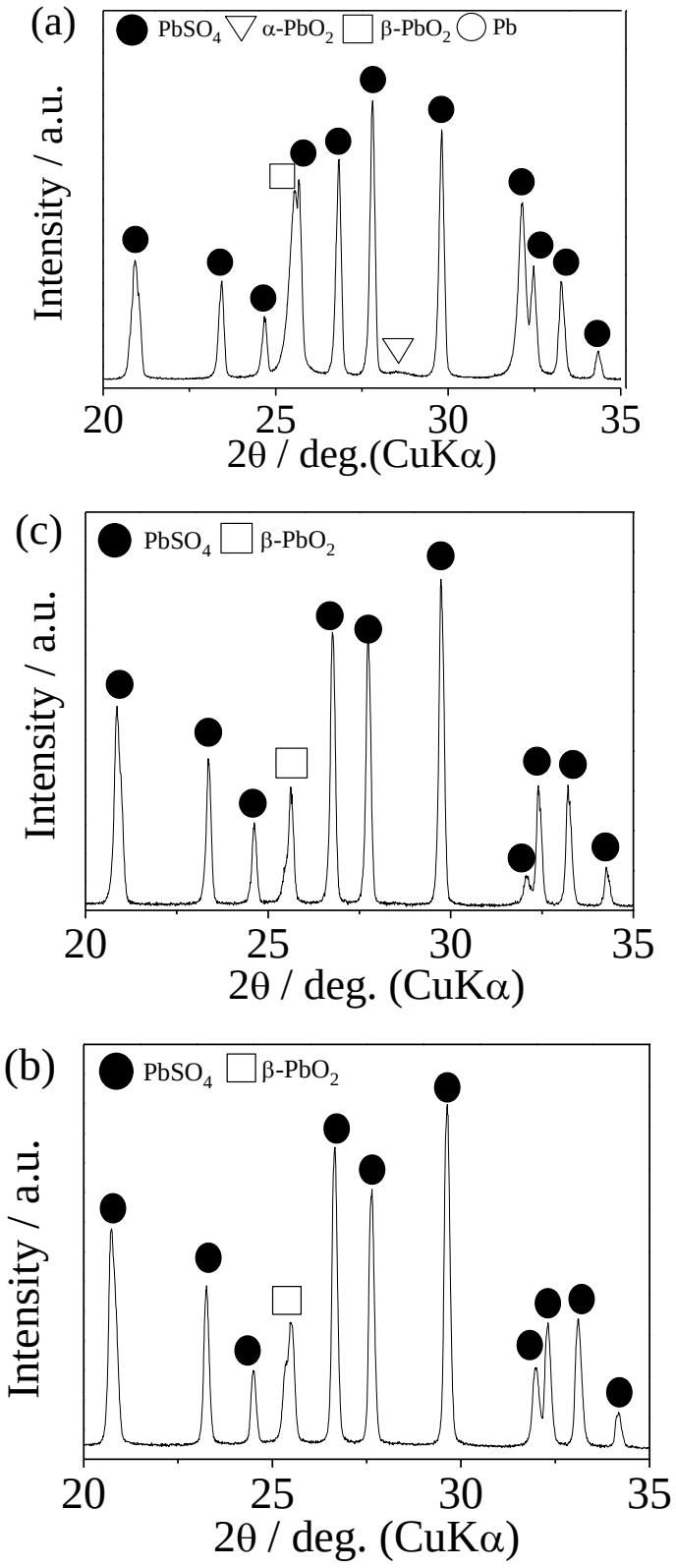

Fig.3-3 XRD patterns of cathode surface after the stabilization process. (a), (b) and (c) show the results for lead plate, gold mesh and platinum mesh, respectively.

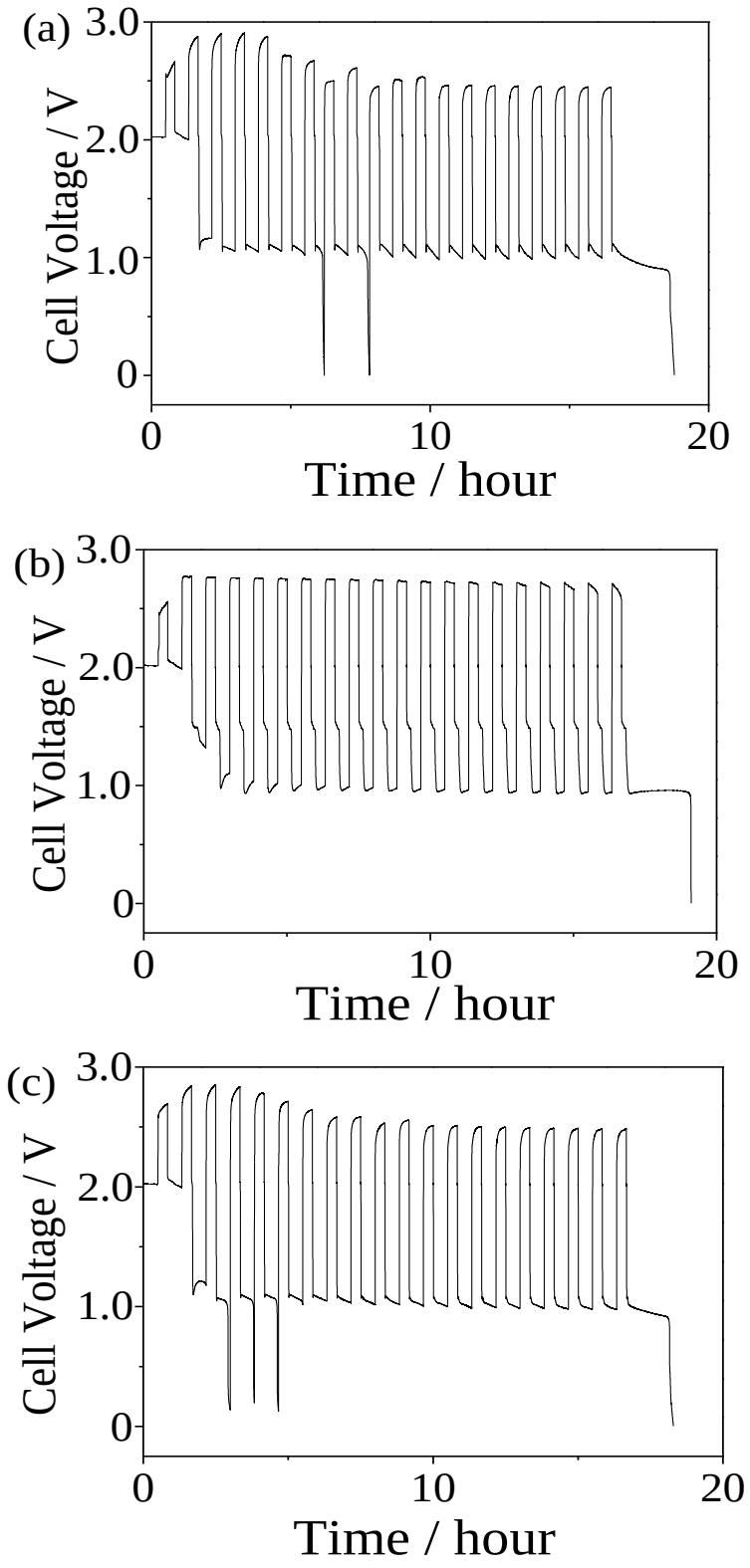

Fig.3-4 Charge-discharge curves of the lead acid battery for the stabilization process and the deep discharge using (a) lead plate, (b) gold mesh and (c) platinum mesh as CCs.

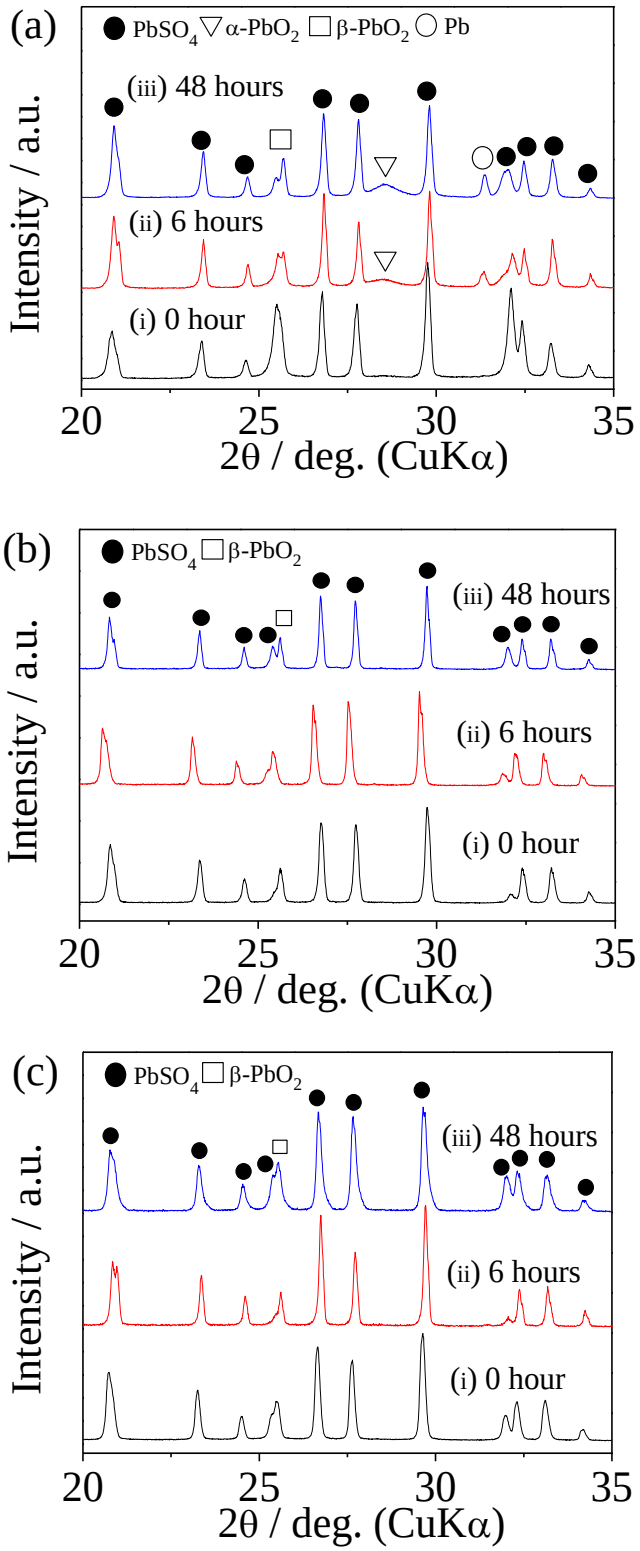

Fig.3-5 XRD patterns of cathode surface. (a), (b) and (c) show the results for lead plate, gold mesh and platinum mesh, respectively. The selected rest time periods are (i) 0 hour, (ii) 6 hours, and (iii) 48 hours.

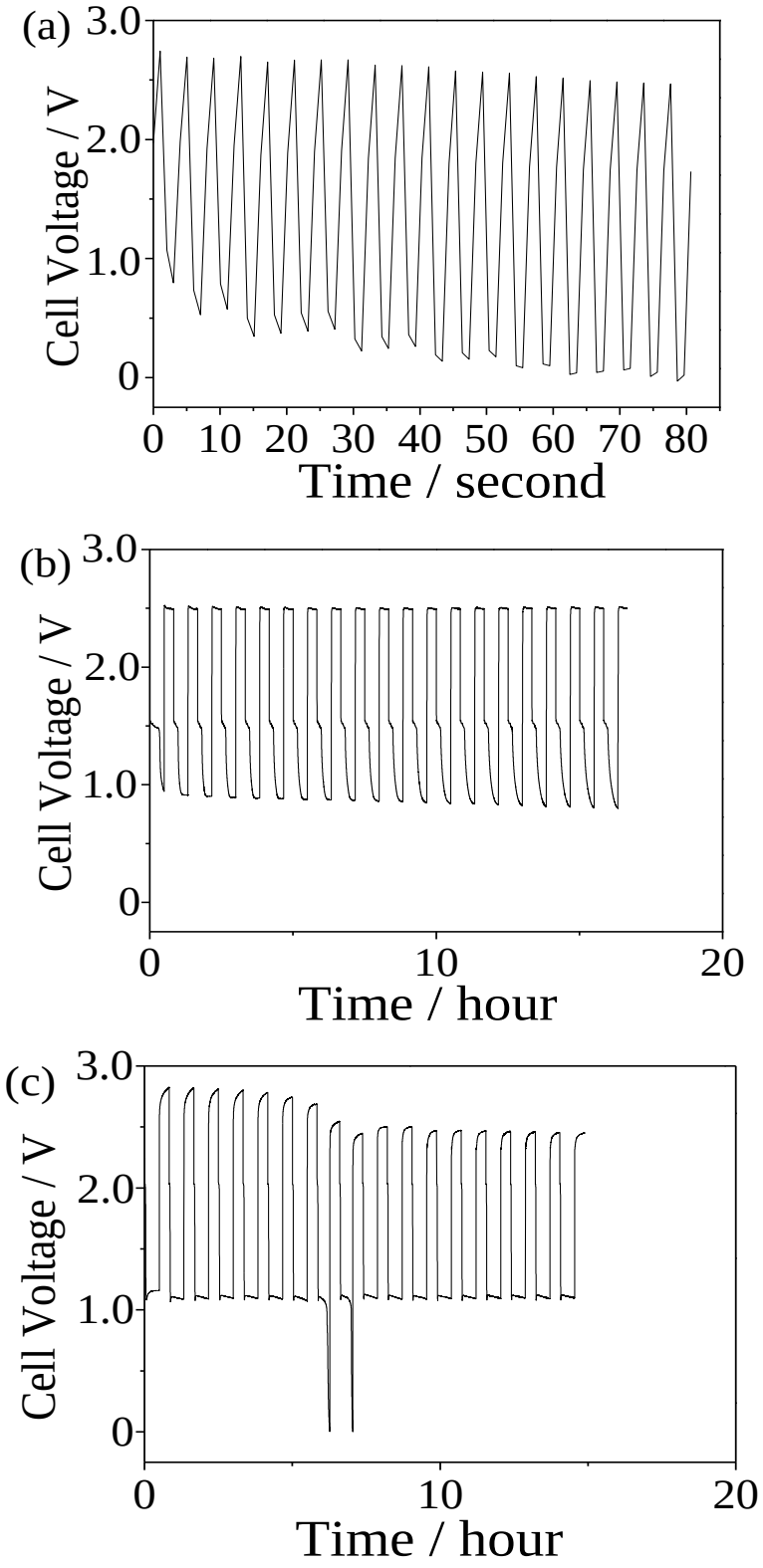

Fig.3-6 Charge-discharge curves of the lead acid battery after the rest time period using (a) lead plate, (b) gold mesh and (c) platinum mesh as CCs.

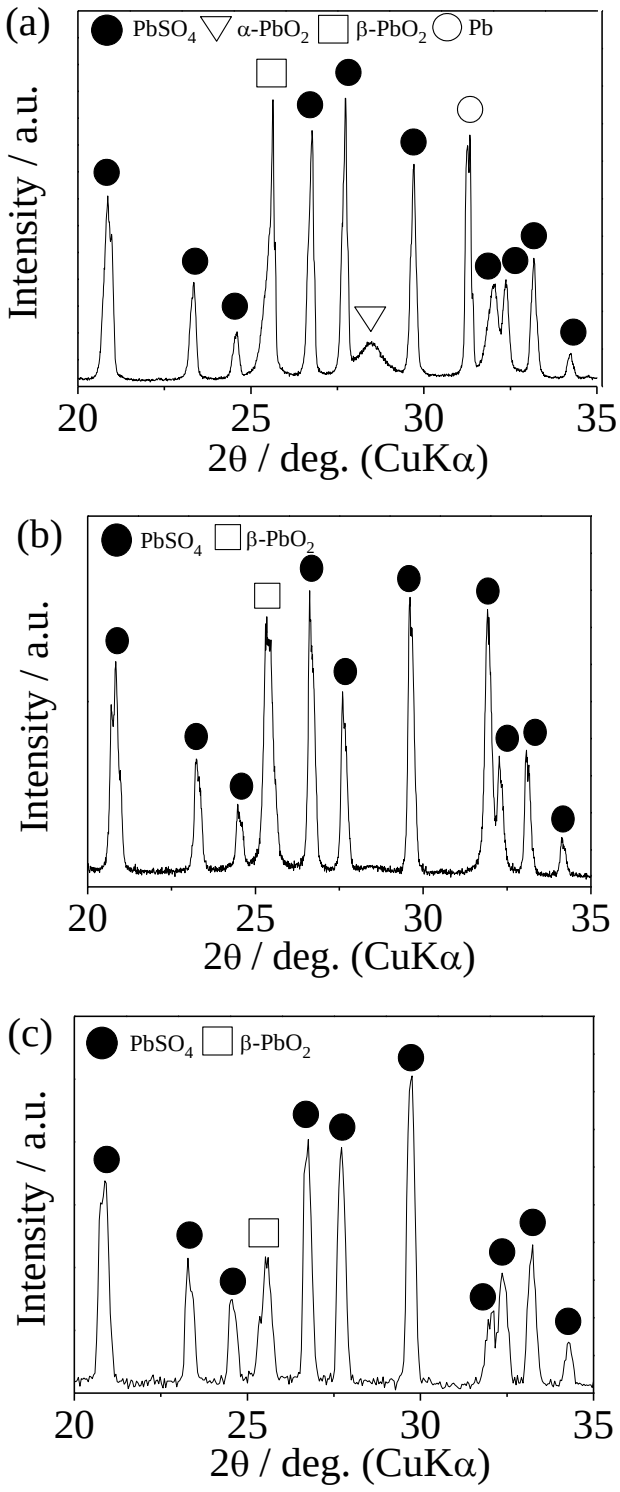

Fig.3-7 XRD patterns of cathode surface after the further charge-discharge cycles. (a), (b) and (c) show the results for lead plate, gold mesh and platinum mesh, respectively.

3.4 Conclusion

In this chapter, the degradation mechanism of lead acid battery caused by the local cell reaction was investigated. After deeply discharging the cell with various CCs followed by leaving the circuit open within 48 hours, X-ray diffraction patterns of cathodes were measured and the charge-discharge ability was examined. Only when the material with lower potential than β-PbO_2 is used as CC, α-PbO_2 phase appears and the cell no longer possesses the charge-discharge ability. It is considered that the reduction of β-PbO_2 occurs due to the local cell reaction to form α-PbO_2, which is different from the previously proposed α-PbO_2 formation model due to the anodic oxidation. The major reason to lose the battery performance is the corrosion of CC due to the local cell reaction.

References

[1] K. Ji, C. Xu, H. Zhao and Z. Dai, *J. Power Sources*, 248 (2014) 307-316. [DOI:

10.1016/j.jpowsour.2013.09.112]

[2] L.C. Peixoto, W.R. Osorio and A. Garcia, *J. Power Sources*, 195 (2010) 621-630. [DOI: 10.1016/j.jpowsour.2009.08.011]

[3] I. Kurisawa, M. Shiomi, S. Ohsumi, M. Iwata, and M. Tsubota, *J. Power Sources*, 95 (2001) 125-129. [DOI: 10.1016/S0378-7753(00)00641-8]

[4] P. Ruetschi and T. Angstadt, *J. Electrochem. Soc.*, 111 (1964) 1323-1330. [DOI: 10.1149/1.2425996]

[5] D. Pavlov, *Electrochimica Acta*, 23 (1978) 845-854.

[DOI: 10.1016/0013-4686(78)87005-4]

[6] D.Pavlov and T. Rogachev, *Electrochimica Acta*, 23 (1978) 1237-1242. [DOI: 10.1016/0013-4686(78)85079-8]

[7] P. Ruetschi and R. T. Angstadt, *J. Electrochem. Soc.*, 105 (1958) 555-563. [DOI: 10.1149/1.2428662]

[8] V. lliev and D. Pavlov, *J. Electrochem. Soc.*, 129 (1982) 458-464. [DOI: 10.1149/1.2123880]

[9] T. Yao, T. Iwai and H. Tagashira, *PCT patent* (2013), PCT /JP2013/ 74165.

[10] I. Petersson, E. Ahlberg, and B. Berghult, *J. Power Sources*, 76 (1998) 98-105. [DOI: 10.1016/S0378-7753(98)00145-1]

Chapter 4 Analysis of the Chemical Change of Cathode Material of Lead Acid Battery before / after Open Circuit

4.1 Introduction

In the previous chapter, the reaction occurred in the cathode of lead acid battery during the rest time was investigated and the performance of the battery was compared by using lead, gold and platinum current collectors (CCs) with different potentials, i.e. the former is lower potential than β-PbO_2 while the latter two are higher. By means of XRD measurements, it has been clarified that the formation of α-PbO_2 occurs after a prolonged rest time only when the lead CC was used. The α-PbO_2 phase creation should be the anodic oxidation of lead oxide in the cathode of lead acid battery as the following model. As the lead sulfate crystals grow to cover the surface of the cathode, and consequently, pH would be increased to form lead oxide in the region between lead sulfate and the CC. The formed lead oxide is then oxidized into α-PbO_2 by the sulfuric acid during the charge process of the battery. Nevertheless, according to this model, anodic oxidation should not occur to form α-PbO_2 during the rest time, for no current flown in the condition of open circuit. Considering the diffraction peak of α-PbO_2 grows larger with increasing the rest time, the local cell reaction (LCR) should bring about the formation of α-PbO_2. To investigate the consistency of above LCR model for α-PbO_2 formation, XPS measurement, SEM observation and impedance measurement were conducted after the deep discharge with the rest time period.

4.2 Experimental

4.2.1 Sample Preparation

Two-electrode glass cell was constructed for charge-discharge experiments. The cathode paste has been prepared by mixing the purchased β-PbO_2 powder (A Johnson Matthey) as an active material, acetylene black as a conducting additive and PTFE as a binder at the weight ratio of 80: 15: 5. Cathode was then fabricated by pressing the paste on a current collector (CC). Three types of CCs i.e. lead plate, gold mesh and platinum mesh, were employed. Lead plate and 30 wt% sulfuric acid (H_2SO_4) were used as the counter

electrode and the liquid electrolyte, respectively.

4.2.2 Impedance Measurements

At first, the cell has been discharged at 9 mAg^{-1} for 30 min and charged at 180 mAg^{-1} for 20 min, which process was cycled for 20 times for the stabilization. Thereafter, the cell was deeply discharged down to 0 V at 9 mAg^{-1}, and then the circuit was opened for 0 to 24 hours because it was revealed that the rest time of 24 hours are enough to form α-PbO_2. The impedance measurement was conducted after the stabilization process, deep discharge down to 0 V, open circuit, respectively. The charge-discharge experiments and impedance measurements were carried out using a potentio-galvanostat (HJ1001SD8, Hokuto; VMP3, Bio-Logic).

4.2.3 XPS Measurements

To investigate the change of the oxidation state and the state of the surface of cathode active material and CC, XPS measurement for Pb 4f emission and SEM observation were conducted before and after the rest time period, respectively. For the XPS measurements, cathode was mounted on a diffractometer (ESCA-750, Shimadzu) and subjected to MgK_α radiation (1253.6eV) for the binding energy range from 130 eV to 160 eV with 0.25 eV step.

4.2.4 Scanning Electron Microscopy

To study the variation of the surface state, SEM (SU6600, Hitachi) investigation was carried out for the interface between cathode active material and CC for (a) lead plate and (b) gold mesh, respectively.

4.3 Results and Discussion

First of all, the charge-discharge process of cells as well as the corresponding XRD patterns are represented to explain the formation of α-PbO_2 phase and cell degradation based on the previous chapter. Fig. 4-1 exhibits the charge-discharge curves at the stabilization process followed by the deep discharge down to 0 V for the cells using (a)

lead plate, (b) gold mesh and (c) platinum mesh CCs. Thereafter the external circuit has been opened for 24 hours and thereafter the charge-discharge experiment was conducted again. While for gold or platinum CCs, charge-discharge experiments are possible after the rest time, this process was no longer available only for the lead CC. Fig. 4-2 shows the XRD patterns of the cathode after the deep discharge followed by 24 hours of the rest period employing (a) lead plate, (b) gold mesh and (c) platinum mesh CCs. Only for the lead plate CC, a diffraction peak around 28° in 2θ was detected as shown in Fig. 4-2(a), which was identified as α-PbO_2 [1-5]. It is thought that the α-PbO_2 was formed due to the reduction of β-PbO_2 due to LCR between β-PbO_2 and CC.

Considering that α-PbO_2 is a slightly reduced form of β-PbO_2 [6-10], the charge state of lead in the cathode active materials as well as lead CC should be evaluated. XPS spectra of cathode active material (PbO_2s) before and after 24 hours of the rest time are represented in Fig. 4-3 for (a) lead plate, (b) gold mesh and (c) platinum mesh CCs. Only for lead plate CC in (a), peak shift of Pb4f toward lower energy direction can be observed, indicating that lead in the active material has been reduced. On the other hand, any apparent change in oxidation states was not detected for (b) gold or (c) platinum CCs, the results of which are consistent with the above local cell reaction (LCR) model. Moreover, XPS spectra for lead CC before and after the rest time are observed in Fig. 4-4. As the peaks shift occurs toward the higher biding energy due to the rest, the lead CC should be oxidized during the rest. Namely, it can be concluded that LCR occurs between β-PbO_2 and lead CC during the rest time.

To investigate the battery degeneration mechanism due to the formation of α-PbO_2 through LCR despite of similar conductivity between α- and β-PbO_2s [11-15], SEM observation has been conducted at the interface of active material and CC. Fig. 4-5 represents the SEM images of the cross-sections of cathodes (a) before and (b) after 24 hours of the rest time. While the flat active material / CC interface was observed in (a), it changed to roughed plane after the rest time in (b). Moreover, some cracks are observed at the interface as well as in active materials with several voids in the CC interior. These voids should be the lead diffusion from CC toward the interface and cracks would be introduced by the volume change for the LCR. Namely in the LCR, the lead supplied

from CC would reduce β-PbO_2 into α-form, oxidizing the supplied lead forming lead oxide. These formed cracks and voids would degrade the battery performance. On the other hand, in the case of gold CC, apparent formation of voids in CC or the growth of lead sulfate which is observed as white crystal were not observed as Fig. 4-6. Accordingly, it is supposed that cracks or voids formed by LCR would cause the degradation of cathode performance.

To investigate the electrochemical contribution of the formed cracks due to LCR, impedance measurements have been conducted. In Fig.4-7, impedance curves before and after the rest time period of 24 hours are shown for (a) lead plate, (b) gold mesh and (c) platinum mesh CCs. For (b) gold mesh and (c) platinum mesh CCs, no apparent increase in impedance was observed or only slight one due to the crystal growth of lead sulfate can be detected. However, for (a) lead plate, drastic increase in impedance is observed in comparison with (b) or (c). Therefore, void or cracks observed in SEM image (Fig.4-5) would enhance the impedance due to the failure of electric contact, resulting in the degradation of the battery.

At the last of this paper, the contribution of the fully discharge process down to 0 V as well as the rest time was investigated from the impedance spectroscopy. Fig.4-8 shows the rest time variation of the impedance curves using lead CC in cathode. For the relatively short rest time as 6 hours, increase in impedance was not observed, while the resistance appeared to increase with rest time as 12 or 24 hours. Accordingly, growth of α-PbO_2 or resulting void / crack formation were thought to proceed in the rest time. As for the contribution of deep discharge process down to 0 V, the impedance after various rest time was compared using the cell without deep discharge treatment. As shown in Fig. 4-9, increase in impedance was not observed even for 24 hours of rest time, indicating that deep discharge process is necessary for the cell degradation phenomena due to the LCR. Considering that α-PbO_2 is the reduced form of β-phase, some content of α-phase is nucleated at the deep discharge, and during the rest time, growth of α-phase accompanied by the void and crack formation would proceed.

In the present study, it was shown that LCR between PbO_2 and CC would occur when the external circuit is open after the deep discharge, resulting in the battery degradation.

In addition, the degradation mechanism was also clarified. For the actual lead acid battery, although growth of lead sulfate at the surface of electrodes is mostly considered, to understand the LCR mechanism during the rest is also significant to improve the battery performance.

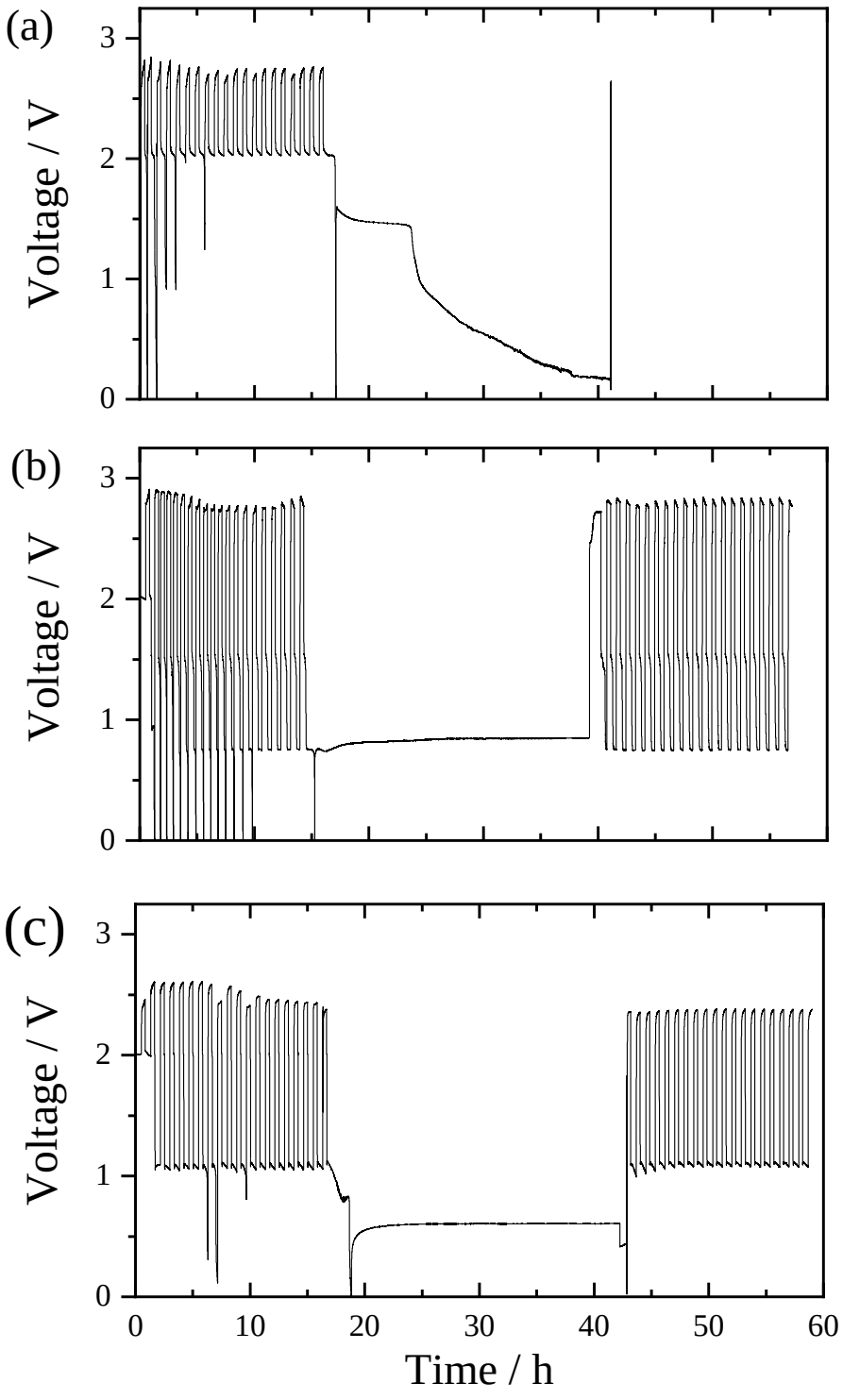

Fig. 4-1 Charge-discharge curves of the lead acid battery after the stabilization process followed by the deep discharge down to 0 V using (a) lead plate, (b) gold mesh and (c) platinum mesh as CCs, respectively.

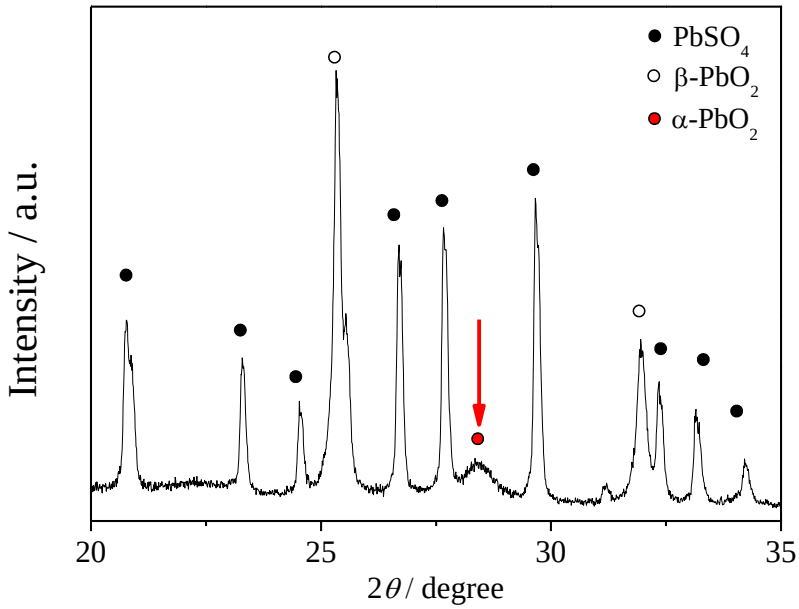
PbSO4
β-PbO2
α-PbO2
Intensity / a.u.
20
25
30
35
2θ / degree

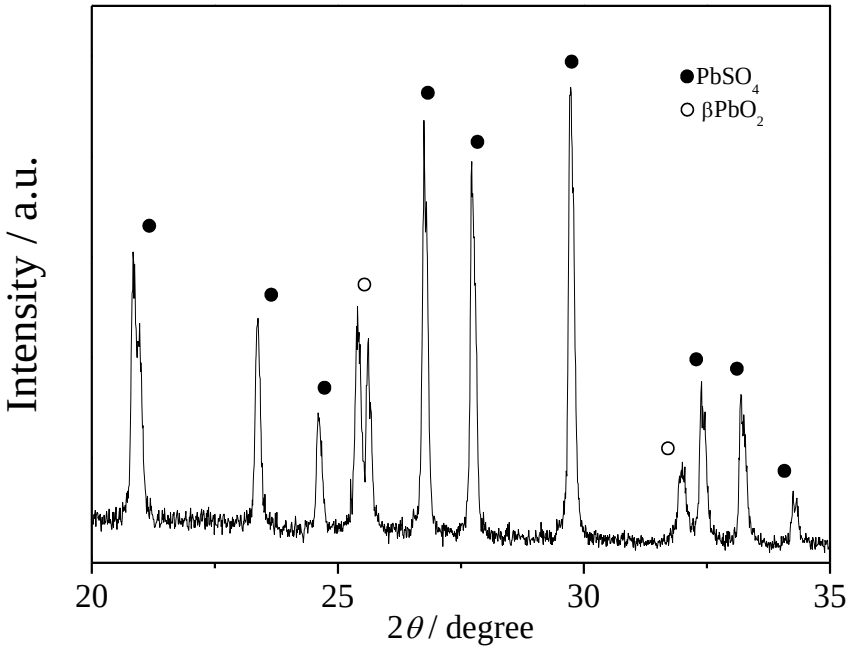
PbSO4
βPbO2
Intensity / a.u.
20
25
30
35
2θ / degree

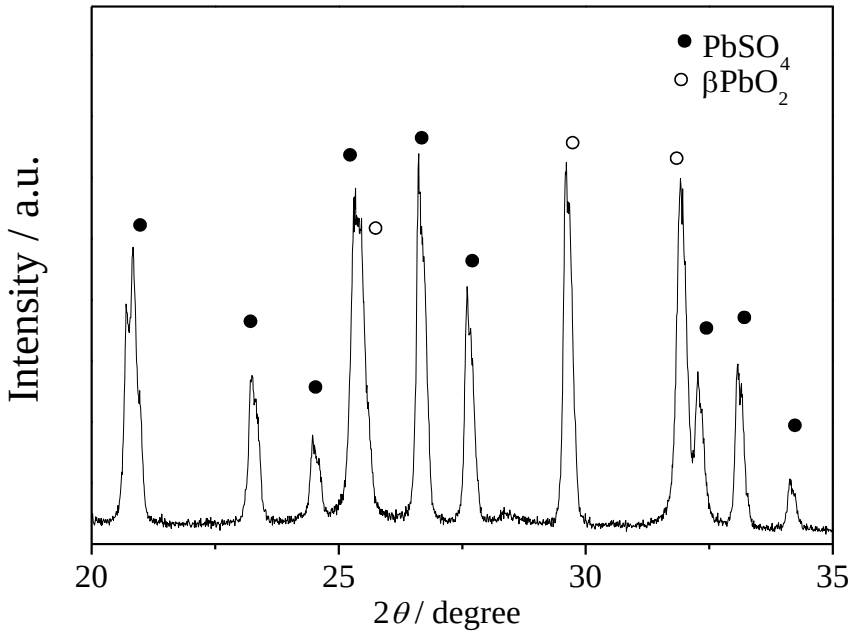

Fig.4-2 XRD patterns of cathode surface after the deep discharge and the rest time period. (a), (b) and (c) represent the results for lead plate, gold mesh and platinum mesh, respectively. The selected rest time periods are (i) 0 hour and (ii) 24 hours.

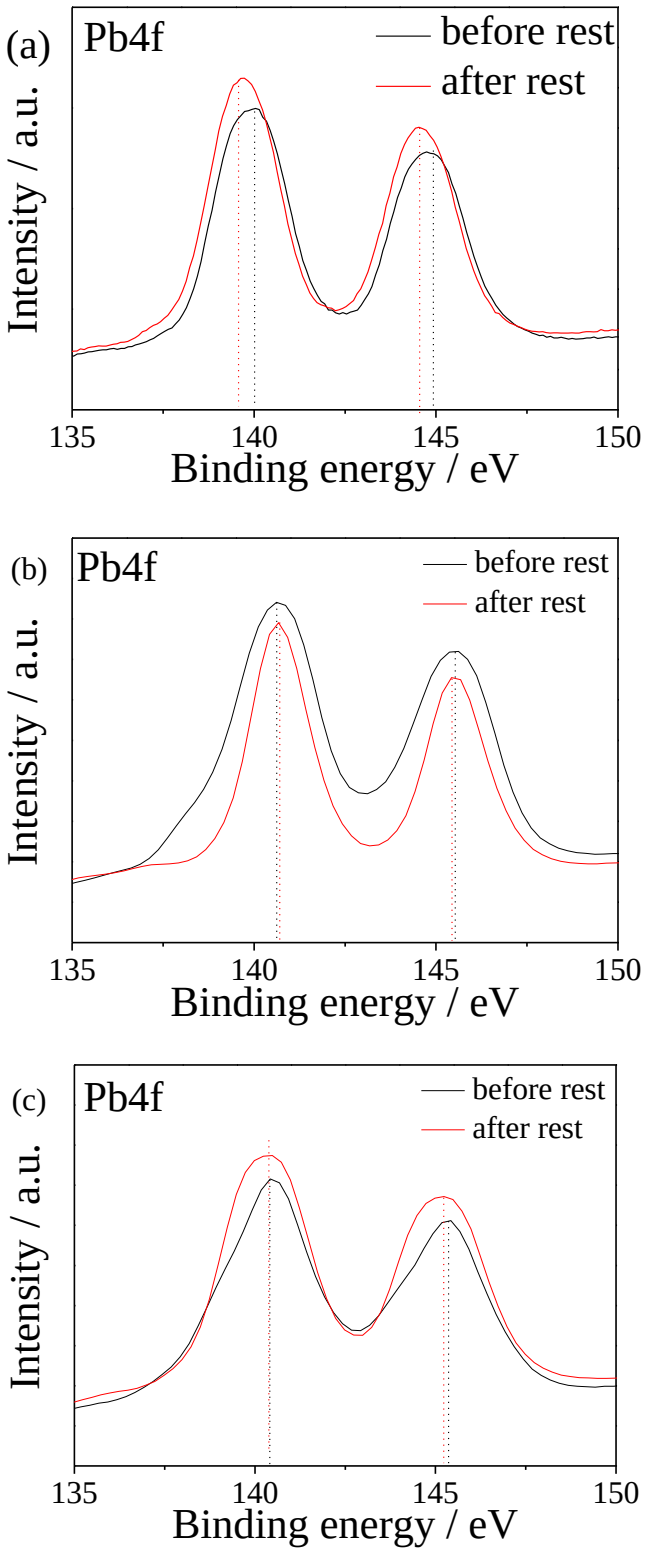

Fig.4-3 XPS spectra of cathode surface before and after the rest time period of 24 hours. (a), (b) and (c) represent the results for lead plate, gold mesh and platinum mesh, respectively.

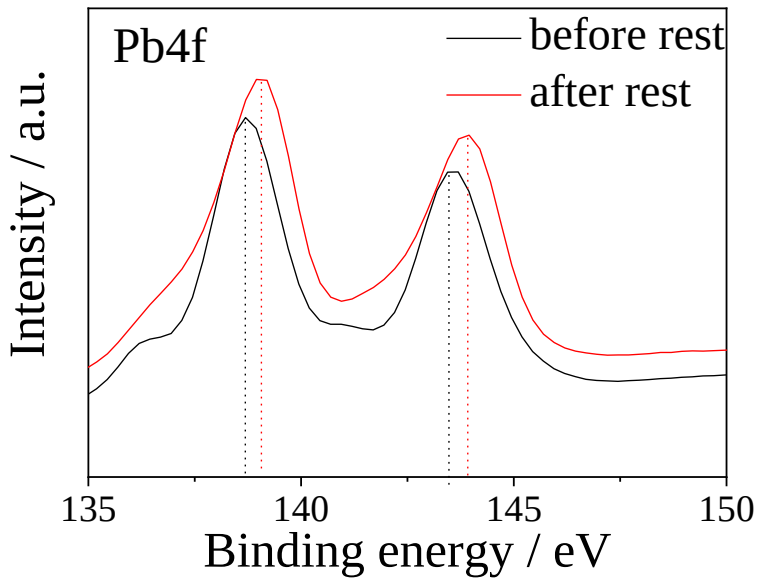

Fig. 4-4 XPS spectra of CC surface for lead plate before and after the rest time period of 24 hours.

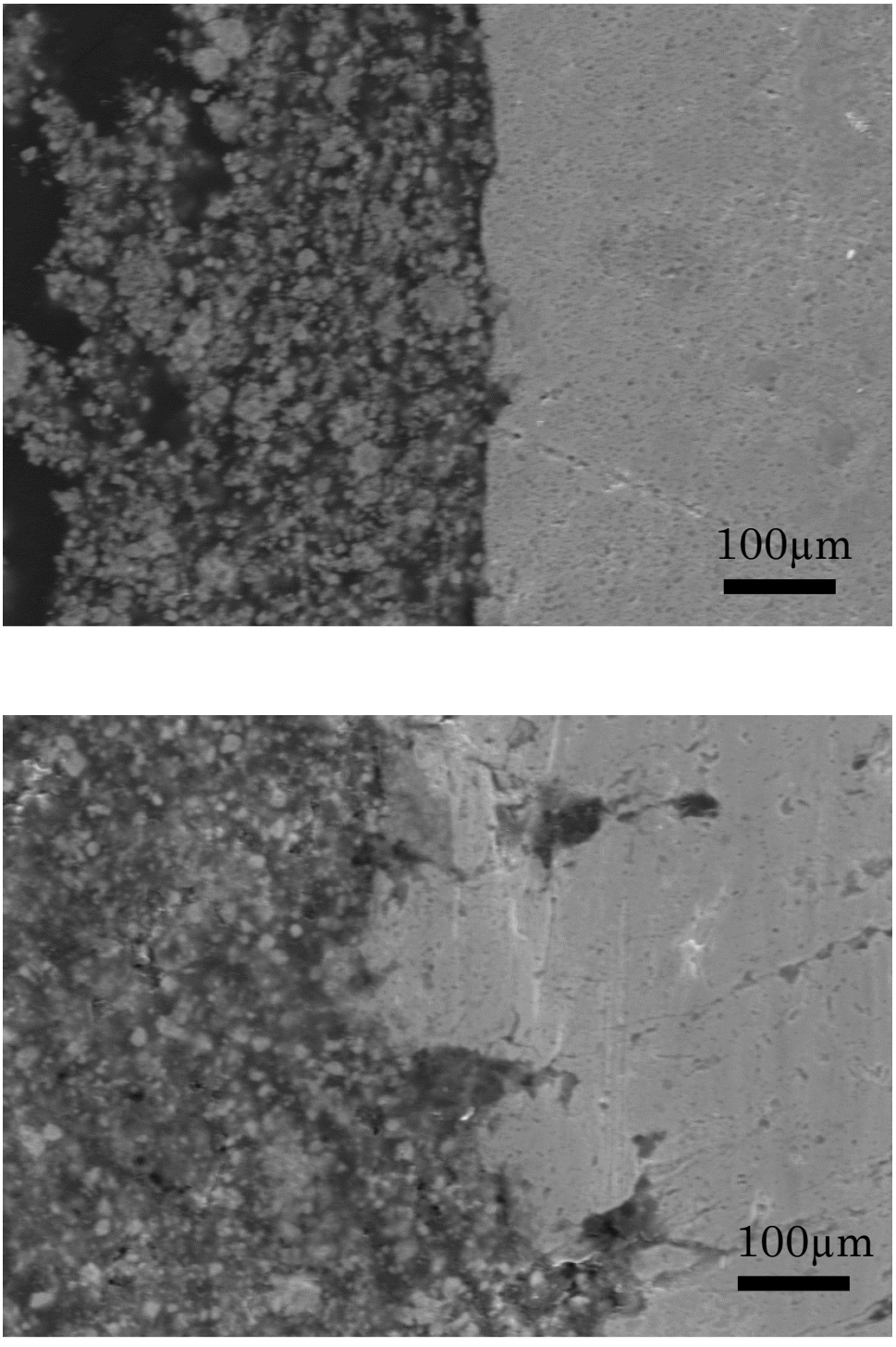

Fig.4-5 SEM images at the interface between cathode active material and lead plate CC (a) before and (b) after the rest time of 24 hours.

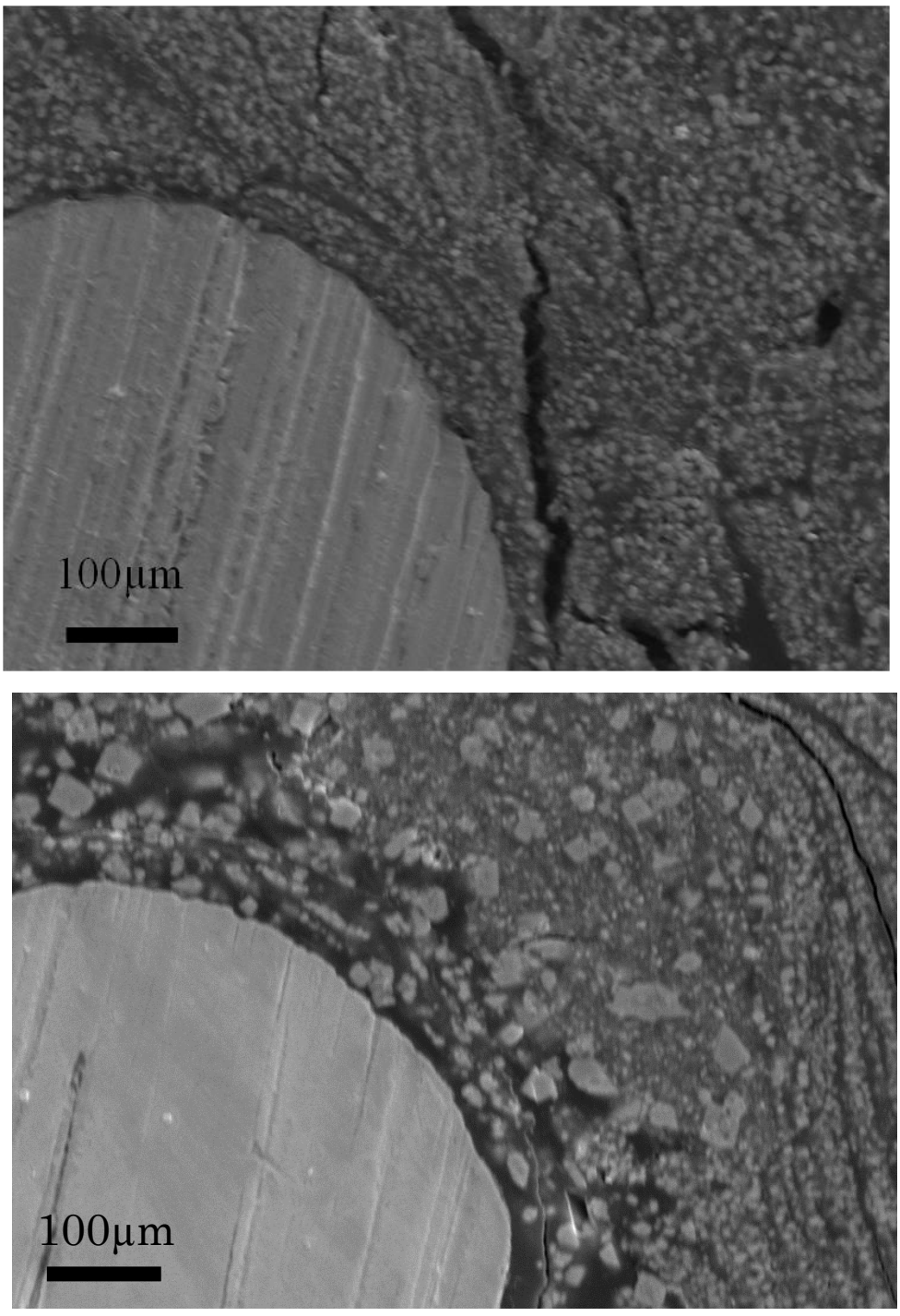

Fig.4-6 SEM images at the interface between cathode active material and gold mesh CC (a) before and (b) after the rest time of 24 hours.

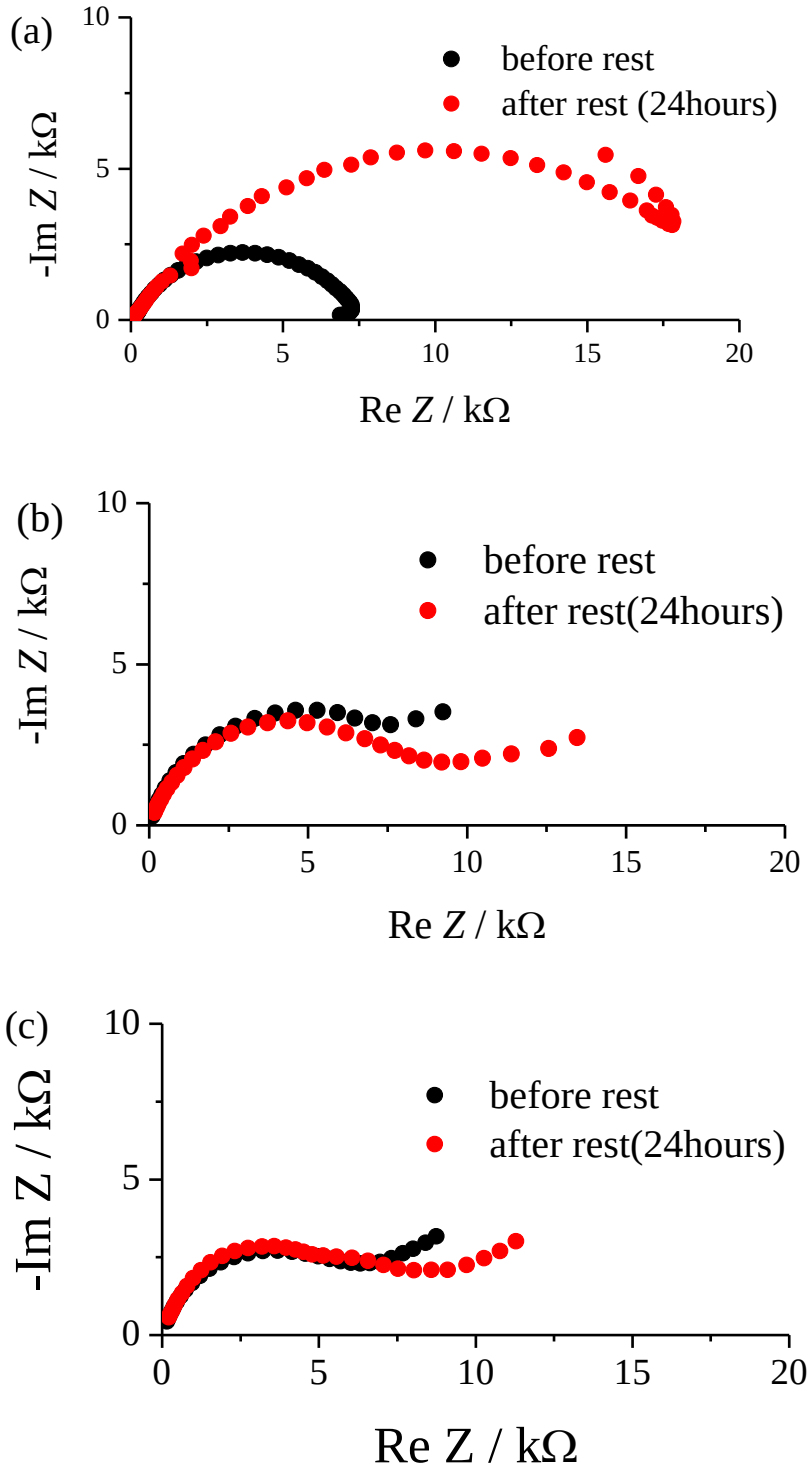

Fig.4-7 Impedance curves of cathode before and after the rest time period of 24hours. (a), (b) and (c) represent the results for lead plate, gold mesh and platinum mesh, respectively.

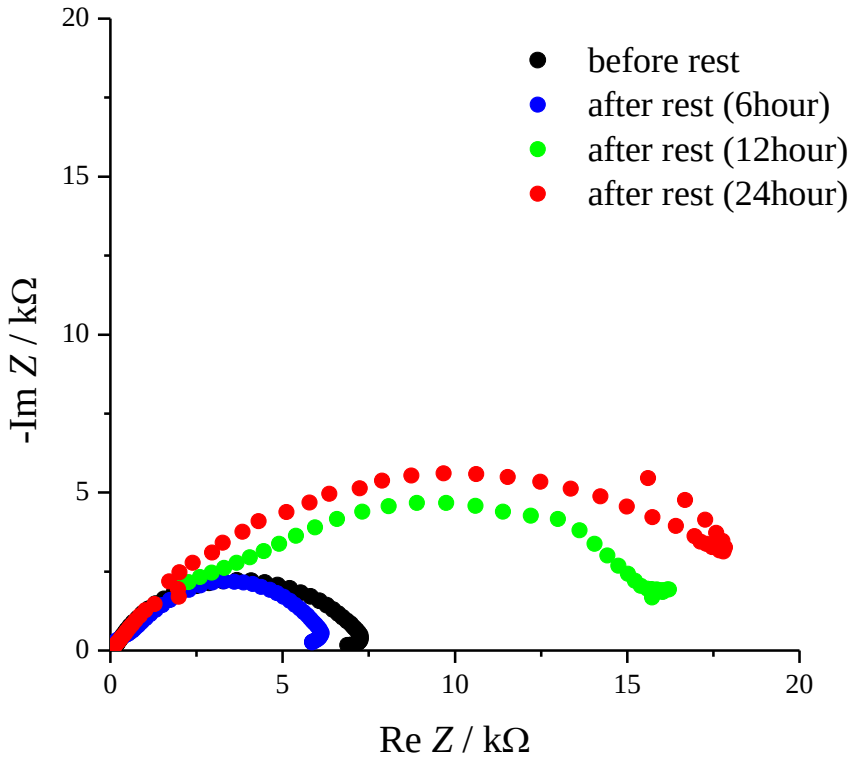

Fig.4-8 Impedance curves of cathode using lead plate CC for the rest time of 0 hour, 6 hours, 12 hours, and 24 hours, respectively.

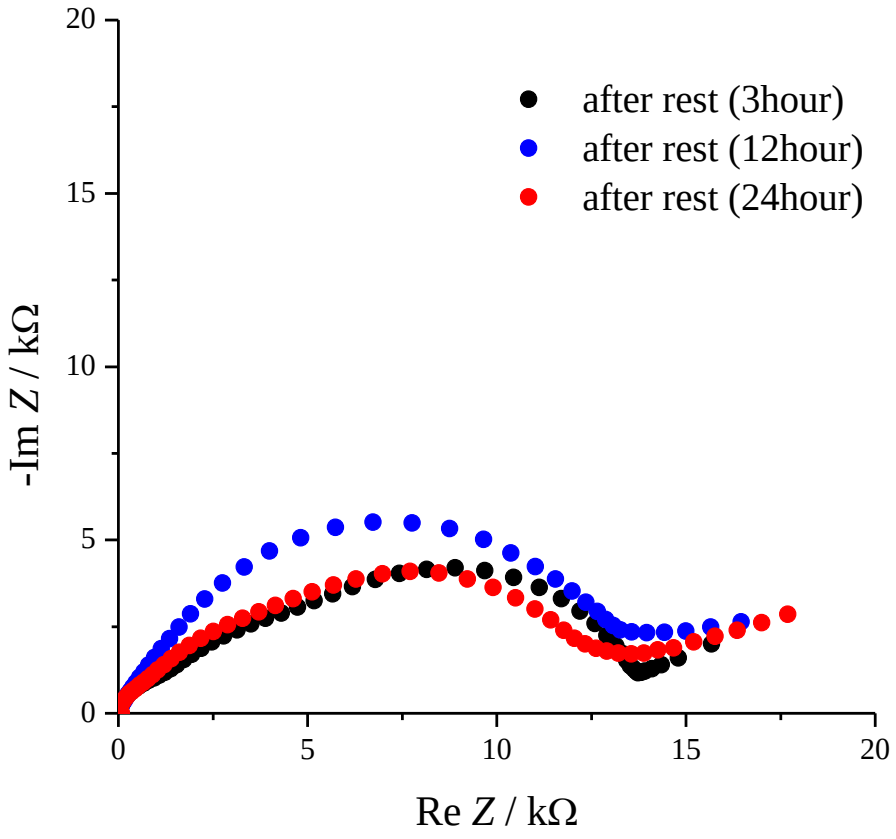

Fig.4-9 Impedance curves of cathode using lead plate CC without the deep discharge down to 0 V for the rest time of 3hours, 12 hours, and 24 hours, respectively.

4.4 Conclusion

In this study, the reaction at the interface between cathode active material and CC was investigated by XPS, SEM, and impedance measurements. Only when the material with lower potential than β-PbO_2 is used as CC after the open circuit of 24 hours, some void in CC and cracks at the cathodes appeared, which leads the critical increase in impedance. It is considered that the void and crack are the major reason for the impedance increase resulting in the critical capacity degradation of the battery. The obtained results were consistent with the LCR model which was proposed in the previous study. It is concluded that the local cell reaction model successfully explains α-PbO_2 formation on the cathode after the deep discharge process down to 0 V and the degradation of the lead acid battery performance during the rest time.

References

[1] A.I. Zaslavsky, Y.D. Kondrashev, S.S. Tolkachev, and D. Akad, *Nauk SSSR*, 75(1950) 559.

[2] A.I. Zalavsky, S.S. Tolkachev, and Z. F. Khimii, *Zh. Fiz Khim.*, 26 (1952) 743.

[3] I. Petersson, E. Ahlberg, and B. Berghult, *J. Power Sources*, 76 (1998) 98-105. [DOI: 10.1016/S0378-7753(98)00145-1]

[4] S. Filatov, N. Bendeliani, B. Albert, J. Kopf, T. Dyuzeva, and L. Lityagina, *Solid State Sciences*, 7 (2005) 1363-1368. [DOI: 10.1016/j.solidstatesciences.2005.08.007]

[5] Z. Chen, Q. Yu, D. Liao, Z. Guo, and J. Wu, *Trans. Nonferrous Met. China*, 23(2013) 1382-1389. [DOI: 10.1016/S1003-6326(13)62607-2]

[6] J. Burbank, *J. Electrochem. Soc.* 111 (1964) 765-768. [DOI: 10.1149/1.2426250]

[7] E.J. Ritchie and J. Burbank, *J. Electrochem. Soc.* 117 (1970) 299-305. [DOI: 10.1149/1.2407498]

[8] H. N. Cong, A. Ejjenne, J. Brenet and P. Faber, *J. Appl. Electrochem*., 11 (1981) 373-386. [DOI: 10.1007/BF00613958]

[9] H. N. Cong and P. Chartier, *J. Power Sources*, 13 (1984) 223-233. [DOI: 10.1016/0378-7753(84)80005-1]

[10] B.M. Chen, Z.C. Guo, X.W. Yang, and Y.D. Cao, *Trans. Nonferrous Met. Soc. China*, 20 (2010) 97-103. [DOI: 10.1016/S1003-6326(09)60103-5]

[11] P. Chartier, *Bull. Soc. Chim. Fr.*, 7 (1969) 2250.

[12] P.Chartier and R. Poisson, *Bull. Soc. Chim. Fr.* 7 (1969) 2255.

[13] K. Nishihara, M. Kurachi, M. Hayashi and T. Hashimoto, *Mem, Fac. Eng. Kyoto Univ*., 152 (1970) 285.

[14] J.P. Pohl and H. Rickert, *Power Sources 5, Academic Press, London,* (1975) 15.

[15] P. Caldara, A. Delmastro, G. Fracchia and M. Maja, *J. Electrochem. Soc.* 127 (1980) 1869. [DOI: 10.1149/1.2130027]

Chapter 5 General Summary

To investigate about the chemical reactions in the battery during open circuit is as important as to study about the performance of the battery in the charge or discharge operation. In this study, the reactions during open circuit and the effect on the battery performance were mainly investigated. By conducting the newly contrived cycle tests with rest time period, local cell reaction (LCR) between the active material and current collector (CC) was intentionally caused, and the effect on the crystal structure of active material and on the battery performance was analyzed.

This thesis is consisted of 5 chapters and chapter 1 is the introduction part.

In chapter 2, the capacity degradation for nickel metal-hydride battery after shallow charge-discharge cycles was investigated. Whereas the formation of γ-NiOOH has been reported to degrade the capacity, its formation mechanism has not been clarified yet. It is thought that LCR between the cathode active material (β-NiOOH) and CC results in the formation of γ-NiOOH to degrade the capacity. By employing three types of CCs, i.e. gold, platinum and nickel meshes, the phase change and capacity loss in terms of LCR. Only for nickel mesh CC were compared. Additional XRD peak around 13° in 2θ occurs accompanied by capacity degradation during charge-discharge cycles, while such phenomena do not for other CCs. This LCR reduces β-NiOOH to transform into a γ-derivative which degrades the battery performance.

In chapter 3, the capacity fading mechanism of the lead acid battery was clarified by focusing on LCR between the cathode active material and CC during the rest time period. Only when the lower potential material in comparison with the cathode active material is employed as CC, formation of α-PbO_2 is detected accompanied by the capacity degradation. It was clarified that LCR of CC results in the α-PbO_2 formation, which correlates with the degradation of the cell performance.

In chapter 4, the coincidence of our LCR model for the degradation mechanism of lead acid battery was confirmed. XPS measurements were carried out to show the reduction of β-PbO_2 into α-form due to the LCR employing various CCs. In addition, impedance spectroscopy and SEM observation revealed that only after discharge down to 0 V followed by opening the circuit, formation of void in the lead CC due to the lead diffusion as well as occurrence of cracks in the cathode active material to form α-PbO_2 by LCR result in the failure of electric contact to degrade the battery performance.

And finally, it is concluded that in the practical battery operation, it is important to design the electrode materials considering local cell reaction. By employing the material

which has the higher potential than the active material, the chemical reaction which causes the degradation of battery performance during the open circuit would be prevented.

List of Publications

This dissertation entitled, “The Degradation Mechanisms of Nickel Metal-Hydride Battery and Lead Acid Battery during Open Circuit” is based on the following publications.

<Chapter 2>

Taichi Iwai, Shigeomi Takai, Takeshi Yabutsuka and Takeshi Yao

“Effect of Local Cell Reaction at Cathode on the Performance of Nickel Metal-Hydride Battery”

J. Alloys and Compounds, Volume 772, Issue 25, Pages 256-262 (2019).

Taichi Iwai, Shigeomi Takai, Takeshi Yabutsuka and Takeshi Yao

“γ-NiOOH formation due to Local Cell Reaction on the Cathode of Nickel Metal-Hydride Battery”

J. Alloys and Compounds, preparing for submission.

<Chapter 3>

Taichi Iwai, Daishi Kitajima, Shigeomi Takai, Takeshi Yabutsuka and Takeshi Yao

“α-PbO_2 formation on the cathode of Lead Acid Battery due to the Local Cell Reaction”

J. Electrochem. Soc., Volume 163, Issue 14, Pages A3087-A3090 (2016).

<Chapter 4>

Taichi Iwai, Masakazu Murakami, Shigeomi Takai, Takeshi Yabutsuka and Takeshi Yao

“Chemical transformation of PbO_2 due to Local Cell Reaction on the cathode of Lead Acid Battery”

J. Alloys and Compounds, Volume 780, Pages 85-89 (2019).

Acknowledgement

I would like to express my deepest gratitude to Emeritus Professor Takeshi Yao of Kyoto University for his valuable and constructive suggestion, and continuous encouragement throughout this study.

I would like to express grateful acknowledgement to Associate Professor Shigeomi Takai of Kyoto University for his valuable discussion and continuous encouragement, which allowed me to carry out the doctor's course. I would like to express thanks to Professor Rika Hagiwara and Professor Takashi Sagawa of Kyoto University for their helpful suggestions, discussions and comments for this study.

I am deeply indebted to Mr. Kitajima Daishi and Mr. Murakami Masakazu. for their technical support and helpful discussions in microscopy observation and analysis of the samples. I gratefully acknowledge Assistant Professor Takeshi Yabutsuka for his technical help on microscopy observation and analysis. I would like to express my deep appreciation to Ms. Megumi Hirose and Ms. Ayaka Kotera, secretaries of Functional Solid State Chemistry Laboratory for a lot helps on studying in the doctor's course. And I would like to thank all the students in Yao laboratory.

Finally, I would like to express my gratitude heartily to my parents, Mr. Nobuhiro Iwai and Ms. Sekiyo Iwai.

March, 2019

Taichi Iwai